Dual role of IFNγ in reprogramming the undifferentiated pleomorphic sarcoma cell line JBT19 towards cytotoxic chemotherapy and antitumor immunity

PAVLA TABORSKA, DMITRY STAKHEEV and DANIEL SMRZ

Department of Immunology, Second Faculty of Medicine, Charles University and University Hospital Motol, 150 06 Prague, Czech Republic

Received May 29, 2025; Accepted November 18, 2025

DOI: 10.3892/ol.2025.15431

Abstract. Soft tissue sarcomas are therapeutically challenging. Among soft tissue sarcoma subtypes, undifferentiated pleomorphic sarcoma (UPS) exhibits one of the most pronounced disparities between its comparatively higher responsiveness to immunotherapy and its limited responsiveness to conventional cytotoxic chemotherapy. The interplay between immunotherapy and cytotoxic chemotherapy is still largely unknown. Interferon-γ (IFNγ) is a key player in antitumor immunity and contributes to the modulation of the tumor microenvironment, which impacts both immune and cancer cells. The mechanism by which this interplay can affect cancer cell chemosensitivity and immune sensitivity is difficult to predict. The present study aimed to investigate the interplay of IFNγ signaling in the UPS cell line JBT19. It was identified that IFNγ treatment significantly decreased the proliferation of JBT19 cells and increased the surface expression levels of cluster of differentiation (CD)44, CD47, CD95 (Fas), major histocompatibility complex (MHC)-I and programmed death-ligand 1 (PD-L1). In addition, IFNγ strongly upregulated surface expression levels of MHC-II and converted JBT19 cells into docetaxel-resistant cells. The IFNγ-induced changes were sustained but reversible after 3 weeks of cell culture without IFNγ. Regardless of IFNγ treatment, JBT19 cells could elicit and amplify the adaptive immune response *in vitro*. The *in vitro* JBT19-reactive lymphocytes effectively eliminated both IFNγ-treated and non-treated JBT19 cells, thus overcoming IFNγ-induced chemoresistance. To the best of our knowledge, the present study demonstrated a dual role of IFNγ towards cancer cell chemoresistance and immunostimulatory potential for the first time. The present study findings may have potential implications for combining immunotherapy with cytotoxic chemotherapy in cancer treatment in the future.

Correspondence to: Dr Daniel Smrz, Department of Immunology, Second Faculty of Medicine, Charles University and University Hospital Motol, V Uvalu 84, 150 06 Prague, Czech Republic
E-mail: daniel.smrz@lfmotol.cuni.cz

Key words: interferon-γ, chemotherapy, immunotherapy, reprogramming, undifferentiated pleomorphic sarcoma

Introduction

Undifferentiated pleomorphic sarcoma (UPS) is an aggressive subtype of soft tissue sarcomas, characterized by a limited response to therapy (1). However, UPS shows higher immunogenicity compared to other sarcoma subtypes, which supports the interest in immunotherapy for this cancer (2). Immunotherapy has changed oncological treatment in recent years, with several patients now receiving it as a first-line therapy (3-6). A number of these therapies, such as immune checkpoint inhibitors, demonstrated notable outcomes for several patients (7). However, for numerous patients, particularly those with solid tumors, immunotherapy still fails and traditional therapeutic modalities, including cytotoxic chemotherapy, need to be used in following therapy lines (8,9). In addition, novel algorithms of oncological treatment may combine multiple therapeutic approaches, such as chemotherapy and immunotherapy or radiotherapy and immunotherapy (10,11). However, despite the progress in the field, how therapeutic combinations may affect each other and the overall therapeutic efficacy remain to be elucidated. One of the key effector molecules associated with immunotherapy is interferon γ (IFNγ) (12). This cytokine is primarily produced by cytotoxic lymphocytes, including cytotoxic cluster of differentiation(CD)8^+ T cells, natural killer (NK) cells and NK T cells, which serve a key role in eliminating cancer cells (13,14). Thus, any treatment leading to the effective removal of cancer cells by cytotoxic lymphocytes is likely to be associated with the production of IFNγ and its collateral impact not only on immune cells (15,16) but also on other cells in the tumor microenvironment, including cancer cells (17-19). Due to the impact of IFNγ on cancer cells, it is difficult to determine how it can affect the efficacy of individual therapeutic approaches or their combinations. Previous studies have reported that IFNγ signatures, patterns of genes, proteins or cellular changes that become activated in response to this cytokine, are frequently associated with enhanced responses to immunotherapy, and elevated IFNγ levels are typically associated with immunotherapy efficacy (20,21). Immunotherapy may sensitize tumors to subsequent chemotherapy (22,23), yet it may also promote resistance to chemotherapy (24,25). This duality implies that IFNγ signatures may likewise exert dual, context-dependent roles across these therapeutic modalities.

UPS is commonly linked to increased infiltration of immune cells (26), which often correlates with IFNγ signatures (27).

However, the specific role of IFNγ in UPS and its implications for immunotherapy and chemotherapy remain unclear. To address this, the present study examined a recently developed, primary tumor-derived, highly transformed, UPS cell line termed JBT19 (28). The present study further explored the mechanism by which prolonged exposure to IFNγ influences the sensitivity of the cell line to cytotoxic chemotherapy and antitumor immunity.

Materials and methods

Cell lines, cell culture and IFNγ-mediated phenotype remodeling. The JBT19 cell line, which originated from a UPS, high-grade soft tissue sarcoma, was established from the primary tumor of a 65-year-old male patient, whose tumor was surgically removed before any other therapeutic interventions and the cell line was subsequently developed using tumor fragmentation-dissociation techniques (28). After 30 passages and >30 months in cell culture, the cell line already exhibited a high population uniformity and was subsequently characterized (28). In the present study, the JBT19 cell line and its green fluorescent protein (GFP)-transfected form (JBT19-GFP) were used after 52 passages and after >35 months in cell culture. The prostate carcinoma cell line PC-3 was used as an epithelial-origin-derived tumor cell line model (29). Cells were adherently cultured (37˚C; 5% CO_2) in RPMI 1640-based FBS-containing complete medium (KM+ medium). KM+ medium consisted of RPMI 1640 medium (Thermo Fisher Scientific, Inc.) supplemented with 10% FBS (non-heat-inactivated; HyClone™; Cytiva), 100 U/ml penicillin-streptomycin, 2 mM GlutaMax, 1 mM sodium pyruvate (Thermo Fisher Scientific, Inc.) and 1 mM non-essential amino acid mix (Thermo Fisher Scientific, Inc.) in tissue culture flasks or plates (TPP Techno Plastic Products AG or SARSTEDT AG & Co. KG). The cells were passaged as previously described using trypsin/EDTA solution (Thermo Fisher Scientific, Inc.) and KM+ medium (28). To reprogram the phenotype of JBT19 cells, the adherent cultured JBT19 cells were supplemented with 200 ng/ml IFNγ (PeproTech, Inc.; Thermo Fisher Scientific, Inc.) for the indicated times. Every 2-4 days, the cells were supplemented with fresh KM+ medium and IFNγ (200 ng/ml). To reverse the phenotype of IFNγ-reprogrammed cells, the cells were extensively rinsed (>3 times) with fresh KM+ medium and cultured for the indicated times. The cells were supplemented with fresh KM+ medium every 2-4 days and/or passaged.

Phenotypic characterization. To evaluate the expression levels of cell surface markers in JBT19 cells, the cells were rinsed with PBS and harvested using trypsin/EDTA solution and KM+ medium. The harvested cells were rinsed with PBS supplemented with 2 mM EDTA (PBS/E) and stained on ice for 30-60 min with the following fluorophore-labeled antibodies: Anti-CD44-Phycoerythrin (PE; clone MEM-263; cat. no. 1P-341-T100; EXBIO Praha, a.s.), anti-CD47-allophycocyanin (APC; clone CC2C6; cat. no. 323124; BioLegend, Inc.), anti-CD95 (Fas)-APC (clone DX2; cat.# 305611; BioLegend, Inc.), anti-fibroblast activation protein (FAP)-α-PE (clone 427819; cat.# FAB3715P-100; R&D Systems, Inc.), anti-CD274 (PD-L1)-APC (clone MIH3; cat.# 374514; BioLegend, Inc.), anti-human leukocyte antigen (HLA)-ABC [major histocompatibility complex (MHC)]-(I)-PE (clone W6/32; cat.# 311406; BioLegend, Inc.) and HLA-DP, DQ, DR (MHC-II)-APC (clone Tü39; cat.# 361714; BioLegend, Inc.). The stained cells were rinsed with PBS/E and supplemented with 100 ng/ml DAPI (Thermo Fisher Scientific, Inc.) shortly before cell analysis. To evaluate the expression levels of intracellular cell markers, the harvested cells were stained on wet ice using LIVE/DEAD Fixable Aqua Dead Cell Stain (Thermo Fisher Scientific, Inc.), fixed and overnight permeabilized as previously described (30). Cells were then stained on wet ice with the following fluorophore-labeled antibodies: Anti-Ki-67-PE (clone Ki-67; cat. no. 1P-155-T100; EXBIO Praha, a.s.), anti-multidrug resistance (MDR)-1-PE (CD243, clone UIC2; cat.# 1P-764-T100; EXBIO Praha, a.s.), anti-B-cell lymphoma (Bcl)-2-PE (clone Bcl-2/100; cat.# 556535; Becton, Dickinson and Company) and anti-signal transducer and activator of transcription (STAT)1-Alexa Fluor 647 (clone 1/STAT1; cat.# 558560; Becton, Dickinson and Company). After staining, cells were rinsed with PBS/E, and the surface of the cells or intracellularly stained cells were analyzed with a FACSAria II or FACSFortesa flow cytometer (Becton, Dickinson and Company). The acquired data were processed using FlowJo software (version 10.10.0; FlowJo LLC; BD Biosciences). The gating strategy used fluorescence minus one staining.

MTT assay, cell cycle assay and annexin V analysis. The cytotoxic impact of treating the cell line with docetaxel, doxorubicin (Selleck Chemicals) or mitomycin C (MilliporeSigma; Merck KGaA), was determined using the MTT assay (MilliporeSigma; Merck KGaA). Briefly, flat-bottom 96-well-cultured adherent JBT19 cells (5,000-20,000 cells/well) were treated with the indicated concentrations of docetaxel, doxorubicin or mitomycin C for 3 days. The cell cultures were then supplemented with 0.5 mg/ml MTT substrate (MilliporeSigma; Merck KGaA) and cultured for 3 h. The supernatant was removed, and the insoluble formazan dissolved with acidified isopropanol (MilliporeSigma; Merck KGaA). The absorbance was acquired at 570 nm and referenced at 630 nm. The acquired data were processed using GraphPad Prism (version 10.2.0; Dotmatics) to determine the half-maximal inhibitory concentration (IC_{50}). Cell cycle analysis was performed as described previously using PI staining (31), with the exception that the data were analyzed using the Dean/Jett/Fox algorithm (docs.flowjo.com/flowjo/experiment-based-platforms/cell-cycle-univariate/) with FlowJo software (version 10.10.0; FlowJo LLC; BD Biosciences). Annexin V staining was performed as described previously (32) using annexin V-FITC (cat. no. EXB0024; EXBIO Praha, a.s.).

Preparation of JBT19-reactive lymphocytes. The source cell material were buffy coats from 4 healthy blood donor volunteers obtained from the Institute of Hematology and Blood Transfusion (Prague, Czech Republic). This material was used to isolate and cryopreserve peripheral blood mononuclear cells (PBMCs) as previously described (30,33). The volunteers provided a prior signed written informed consent for the use of the biological material for research. The research adhered to the ethics standards of the institutional research committee

and was approved by the Ethics Committee of the University Hospital Motol in Prague (approval no. EK-602.4/22; Prague, Czech Republic). The research was performed in compliance with the 1964 Helsinki Declaration and its later amendments. The JBT19-reactive lymphocytes were produced as described previously (28) with minor modifications. Briefly, the cryopreserved PBMCs were reconstituted overnight (2-3x10^6 cells/ml) in RPMI 1640-based human serum-containing complete medium [lympho medium (LM), consisting of RPMI 1640 medium (Thermo Fisher Scientific, Inc.) containing 5% human serum (One Lambda, Inc.; Thermo Fisher Scientific, Inc.) and other non-serum supplements as in KM+ medium] supplemented with human IL-2 (500 IU/ml; PeproTech, Inc.; Thermo Fisher Scientific, Inc.). The reconstituted cells were harvested, pelleted and reconstituted in fresh LM with 500 IU/ml IL-2 at 4x10^6 cells/ml. The cells were then combined at a 1:1 ratio with trypsin/EDTA-harvested and UV-inactivated (312 nm; 2.55 J/cm^2) JBT19 cells that were previously treated or not with 200 ng/ml human IFNγ for 7 days (1x10^6 cells/ml) [final ratio, 4:1 (PBMC/JBT19)]. The combined cells were cultured in a flat-bottom 48-well plate well (Nalgene; Thermo Fisher Scientific, Inc.). On days 3, 5 and 6, the cell cultures were hemi-depleted and supplemented with fresh LM and 500 IU/ml IL-2. On day 7, the cell cultures were transferred to a flat-bottom 12-well plate well (Nalgene; Thermo Fisher Scientific, Inc.) and supplemented with an equal volume of fresh LM and 500 IU/ml IL-2. On days 10 and 11, the cell cultures were hemi-depleted and supplemented with fresh LM and 500 IU/ml of IL-2. On day 12, the cells were analyzed and/or cryopreserved.

Rapid expansion protocol (REP) for JBT19-reactive lymphocytes. The 12-day cryopreserved cell cultures enriched with lymphocytes reactive to JBT19 cells or IFNγ-treated JBT19 cells were reconstituted as aforementioned in LM with 500 IU/ml IL-2. The reconstituted cells were then large-scale expanded for 14 days using an REP as previously described (34), with the exception that following the initial IL-2 concentration of 4,000 IU/ml, the cells were next cultured with 2,000 IU/ml IL-2. On day 14, the large-scale expanded cells were analyzed and/or cryopreserved.

Analyses of JBT19-reactive lymphocytes. The cultured lymphocytes (enriched or large-scale expanded) were analyzed with small modifications using procedures described previously (28). Briefly, the cultured lymphocytes were harvested, pelleted and resuspended in fresh LM with 500 IU/ml IL-2 at 4x10^6 cells/ml. The lymphocytes were then combined at a 1:1 ratio with trypsin/EDTA-harvested JBT19 cells treated or not with 200 ng/ml IFNγ for 7 days [1x10^6 cells/ml; final ratio, 4:1 of lymphocytes (effector)/JBT19 (target)]. The combined cells were then transferred to a U-bottom 96-well plate (Nalgene; Thermo Fisher Scientific, Inc.) and cultured (stimulated) at 37˚C in the presence of 5% CO_2. After 1 h, the cells were supplemented with Brefeldin A (BioLegend, Inc.) to prevent cytokine secretion from the cells and cultured for an additional 4 h. The cells were transferred to a V-bottom 96-well plate (Nalgene; Thermo Fisher Scientific, Inc.), pelleted, rinsed with PBS/E and stained on wet ice with LIVE/DEAD Fixable Aqua Dead Cell Stain (Thermo Fisher Scientific, Inc.). The stained cells were next fixed, overnight permeabilized and stained on wet ice with anti-CD3-peridinin-chlorophyll-protein-cyanine (Cy)5.5 (clone SK7; cat. no. T9-173-T100), anti-CD4-PE-Cy7 (clone MEM-241; cat. no. T7-359-T100), anti-CD8-Alexa Fluor 700 (clone MEM-31; cat. no. A7-207-T100; EXBIO Praha, a.s.), anti-TNFα-APC (clone monoclonal antibody 11; cat.# 562084) and anti-IFNγ-PE (clone B27; cat.# 559327; Becton, Dickinson and Company) antibodies. The stained cells were pelleted, rinsed with PBS/E and analyzed by flow cytometry as aforementioned. Reactive cell frequency was calculated as the difference between the proportion of IFNγ- and/or TNFα-producing cells in the JBT19 cell-stimulated sample and the corresponding vehicle-stimulated control from the same sample. In certain experiments, lymphocytes were pretreated for 30 min with 20 μg/ml anti-MHC-I (clone W6/32; cat. no. 311428; BioLegend, Inc.) or anti-MHC-II (clone Tü39; cat.# 555556; Becton, Dickinson and Company) blocking antibodies in serum-free RPMI 1640 medium (Thermo Fisher Scientific, Inc.) and then stimulated in the presence or absence of 10 μg/ml antibodies in LM. The flow cytometry was performed as aforementioned.

Analysis of the cell-mediated cytotoxic impact on JBT19-GFP cells. JBT19-GFP cells were generated as previously described (28). The cytotoxic impact of lymphocytes (enriched or large-scale expanded) on JBT19-GFP cells treated or not with 200 ng/ml IFNγ for 7 days was assessed using a previously described protocol with a small modification (28,35). Briefly, 0.1x10^6 JBT19-GFP cells (target) were passaged into a flat-bottom 48-well plate well and cultured for 1 day. Upon supernatant removal, the wells were supplemented with 1.0 x10^6 lymphocytes (effector) in 1 ml LM with IL-2 (500 IU/ml). After lymphocyte sedimentation for 10 min, the fluorescence of JBT19-GFP cells in the wells was acquired with a fluorescence microscope and the mean fluorescence intensity (MFI) at day 0 was calculated using image analysis with ImageJ 1.44p (National Institutes of Health) as previously described (36). The cells were cocultured for 3 days and MFIs were determined as on day 0.

Statistical analysis. Values were calculated from the *n* sample size using GraphPad Prism 10.2.0 (GraphPad; Dotmatics). Data are presented as the mean ± SEM of ≥3 independent experimental repeats. Differences between groups were determined with the indicated paired or unpaired two-tailed Student's t-test or with one-way ANOVA followed by Tukey's post hoc test. $P<0.05$ was considered to indicate a statistically significant difference, unless indicated otherwise.

Results

IFNγ abrogates in vitro proliferation of JBT19 cells, increases their expression levels of CD44, CD47 and CD95 (FAS) and induces docetaxel resistance. IFNγ is a cytokine produced by activated NK cells and cytotoxic $CD8^+$ T cells (13). These cells are key effector cells responsible for cancer cell elimination (14,37) and their presence in tumors is often associated with improved prognosis of the disease (38,39). However, once released in the tumor microenvironment, its chronic impact can also modulate cancer cells. Therefore, the present

study used the recently established UPS sarcoma cell line JBT19 (28) and investigated the long-term (chronic) impact of this cytokine on the proliferation and phenotype of JBT19 cells. The rationale for using this cell line was based on the observation that, although two-dimensional-cultured JBT19 cells exhibited little-to-no surface expression levels of MHC-II molecules, as determined by flow cytometry, supplementation of the culture medium with IFNγ for 3 days induced robust surface expression levels of MHC-II (Fig. 1A). This response was concentration dependent, reaching a plateau at concentrations >5 ng/ml (Fig. 1B). Furthermore, IFNγ supplementation reduced the proliferation of JBT19 cells. To further investigate this effect, JBT19 cells were cultured in the presence of 200 ng/ml IFNγ for 7 days, ensuring a robust and stable response within the plateau range and cell proliferation was subsequently evaluated in the presence or absence of the cytokine. After the initial delay in the cell proliferation in the first 3 days, presumably due to a transient adverse impact of the passaging procedure on cell proliferation, IFNγ markedly suppressed the proliferation of JBT19 cells, increasing their doubling time >3-fold, from ~2 to >6 days (Fig. 1C and D). This suppression led to a marked decrease in the proliferation of the cell culture. Whereas the non-treated cell culture exhibited a 150-200-fold increase in cell numbers in 12 days, cells treated with IFNγ expanded 3-4-fold.

Next, the present study investigated how this marked decrease in JBT19 cell proliferation affected the expression levels of cell surface markers, which are reported to be possibly associated with modulated resistance of cancer cells to the immune system and chemotherapeutics. Among these markers were CD44 (which is associated with cancer cell stemness), CD47 (a receptor inhibiting phagocytosis by macrophages and its expression in multiple cancer types, such as in ovarian and gastric cancer, is associated with chemoresistance and poor prognosis) (40-42) and CD95 (Fas; a death receptor inducing apoptosis) (43). As shown in Fig. 1E, 7-day treatment of JBT19 cells with IFNγ increased the surface expression levels of CD44, CD47 and CD95 (Fas) in JBT19 cells. By contrast, the surface expression levels of FAP were reduced. These results demonstrated that IFNγ suppressed the proliferation of JBT19 cells but induced a phenotype that could possibly affect JBT19 cell resistance to cytotoxic chemotherapy and immunotherapy.

The IFNγ-mediated inhibition of JBT19 cell proliferation suggested that these cells may develop resistance to chemotherapeutic agents that primarily target dividing cells (44). Therefore, the present study next examined the cytotoxic effects of docetaxel on IFNγ-treated JBT19 cells. Docetaxel is a commonly used chemotherapy drug (45) that targets dividing cells by inhibiting the depolymerization of microtubules, causing mitotic arrest and subsequent apoptosis (46). JBT19 cells were sensitive to docetaxel at nanomolar (nM) concentrations (IC_{50}=14.98 nM) as determined by MTT assay (Fig. 1F). However, 7-day treatment of these cells with IFNγ made these cells highly resistance to docetaxel (Fig. 1G), decreasing their sensitivity by >2,000-fold (IC_{50}=38.71 μM; Fig. 1H). These results demonstrated that, albeit IFNγ nearly blocked the proliferation of JBT19 cells, this was associated with the acquisition of chemoresistance to a widely used drug such as docetaxel, to which JBT19 cells were otherwise sensitive at nM concentrations.

IFNγ changes the cell cycle, does not induce apoptosis and increases STAT1 expression without inducing the surface expression levels of multidrug resistance protein 1 (MDR-1) or enhancing the expression levels of Bcl-2 in JBT19 cells. IFNγ treatment is known to impact the cell cycle (47); therefore, it was next examined how the 7-day IFNγ treatment affected the cell cycle of JBT19 cells. The results revealed a trend toward increased frequencies of cells in G_1 and G_2 phases and a decreased frequency in the combined G_2 + S population. Notably, IFNγ treatment induced a significant reduction in the proportion of cells in S phase (Fig. 2A and B). This pattern of IFNγ-mediated cell cycle changes was consistent with observations in other cell types (48,49). The treatment of JBT19 cells with IFNγ was not associated with increased apoptosis, expression levels of MDR-1 receptor (50) or modulation of the expression levels of the antiapoptotic signaling molecule Bcl-2 (51) (Fig. 2C-G). However, sustained exposure to IFNγ for 7 days enhanced the expression levels of the STAT1 signaling molecule (Fig. 2H), a response previously reported in multiple cell types (52-55).

IFNγ decreases the expression levels of Ki-67 and increases the expression levels of PD-L1 and MHC-II in JBT19 cells. The marked impact of IFNγ on the performance of JBT19 cells towards chemoresistance was associated with long-term (7-day) exposure of JBT19 cells to this cytokine. The present study next evaluated a shorter exposition of JBT19 cells to this cytokine and investigated a possible reversibility of its effect on their proliferation. To do that, Ki-67 was used as a surrogate marker of cell proliferation (56). Ki-67 expression was analyzed in JBT19 cells treated with IFNγ (200 ng/ml) for 7 days, 2 days or 2 days followed by its extensive removal and additional 5-day cell culture. As shown in Fig. 3A-C, 2-day IFNγ treatment decreased the levels of Ki-67 nearly to the levels observed in 7-day treated cells. Furthermore, these levels were sustained even after the following 5 days of cell culture in the absence of IFNγ. These findings demonstrated that the anti-proliferative impact of IFNγ on JBT19 cells was induced after a shorter time exposure but was not reversed even 5 days later.

The sustained IFNγ-mediated inhibition of JBT19 cell proliferation suggested that their phenotype could also be maintained in the absence of IFNγ. However, since the IFNγ-induced differences in the surface expression levels of the previously investigated markers [CD44, CD47, CD95 (Fas) and FAP] were not extensive, the investigation next focused on other possible markers whose expression was previously reported to be sensitive to IFNγ treatment, including PD-L1 (19), MHC-I (57) and MHC-II (58). The first two markers were cell surface-expressed in JBT19 cells and the expression levels of MHC-II were found to be significantly expressed after IFNγ treatment in the present study. In these experiments, JBT19 cells were treated with IFNγ as for the Ki-67 analyses and the cell surface expression levels of PD-L1, MHC-I and MHC-II was determined. As shown, although JBT19 cells were previously reported to be PD-L1$^+$ (28), the increase in PD-L1 expression after treatment with IFNγ was robust (Fig. 3D). Similar to Ki-67, the expression levels of PD-L1 was the highest after 7 days of treatment. However, notable differences were observed compared with the impact on Ki-67 expression.

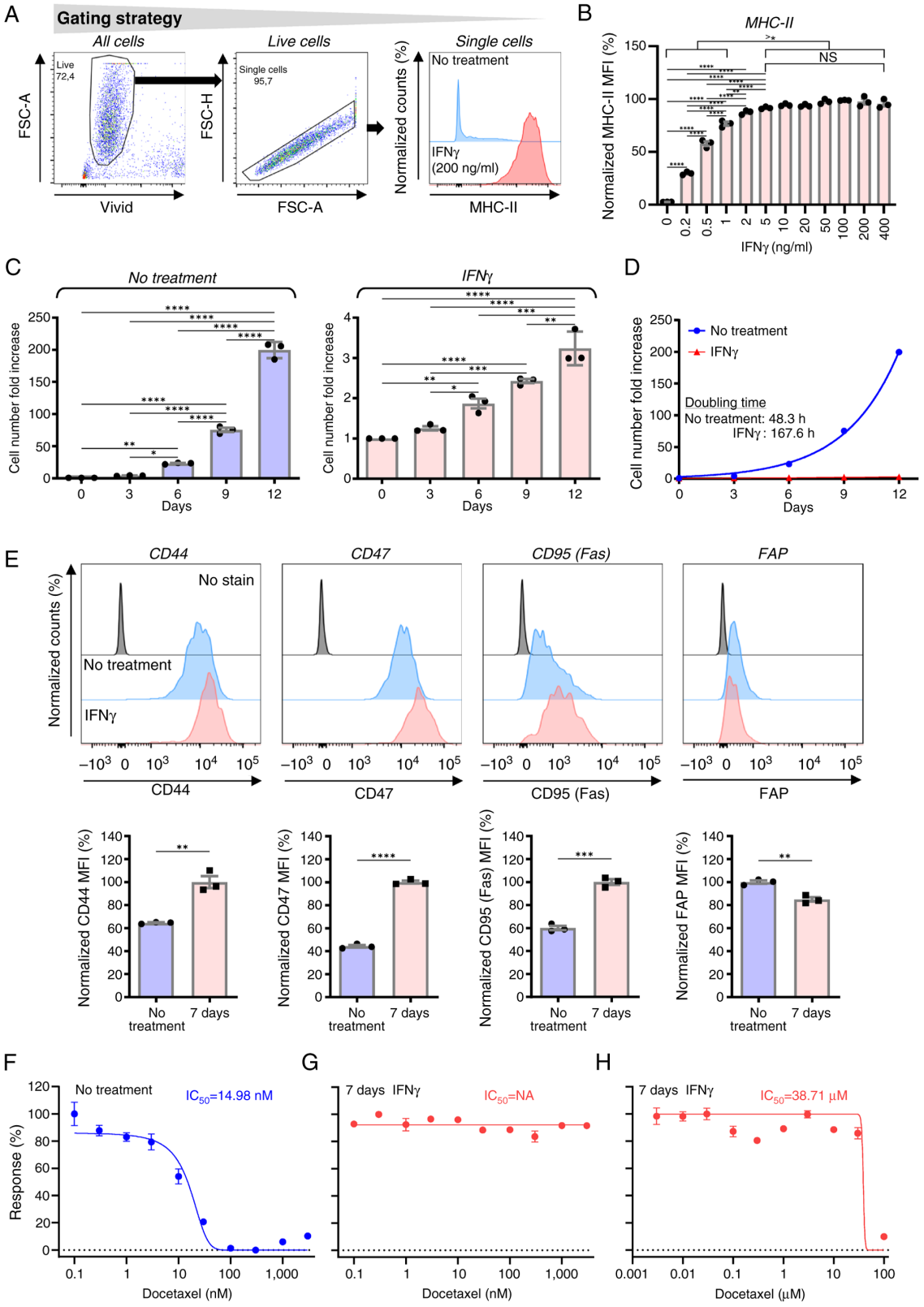

Figure 1. Impact of IFNγ on the *in vitro* proliferation of JBT19 cells and their expression levels of MHC-II, CD44, CD47 and CD95 (Fas), and their sensitivity to docetaxel. (A) Gating strategy of flow cytometry data. (B) Extracellular MHC-II staining of 3-day treated JBT19 cells with the indicated concentrations of IFNγ. (C) Cell number fold increase in vehicle-treated JBT19 cells (No treatment, left panel) or 7-day pre-treated and then cultured with IFNγ (200 ng/ml; IFNγ, right panel). The evaluated are represented as means ± SEM. *P<0.05, **P<0.01, ***P<0.001 and ****P<0.0001; n=3 independent experiments; one-way ANOVA with Tukey's post hoc test). (D) Calculated proliferation curves and pertinent doubling times from the data shown in panel C. (E) Extracellular staining of 7-day vehicle-treated (No treatment) or 7-day IFNγ-treated (IFNγ, 200 ng/ml) JBT19 cells. The cells were stained with specific antibodies against CD44, CD47, CD95 (Fas) or FAP. In the top panels, representative histograms are shown and the control (No stain) for individual fluorochromes refers to staining with vehicle alone. In the bottom panels, the evaluated data presented as means ± SEM are shown and statistically significant differences between the groups are indicated. **P<0.01, ***P<0.001 and ****P<0.0001. MTT assay of (F) vehicle-treated JBT19 cells (No treatment), or (G and H) 7-day IFNγ-treated (IFNγ, 200 ng/ml) JBT19 cells (7 days IFNγ) exposed to docetaxel at the indicated concentrations for 3 days. The calculated IC_{50} from three independent experiments is shown. MFI, mean fluorescence intensity; MHC, major histocompatibility complex; nM, nanomolar; FAP, fibroblast activation protein.

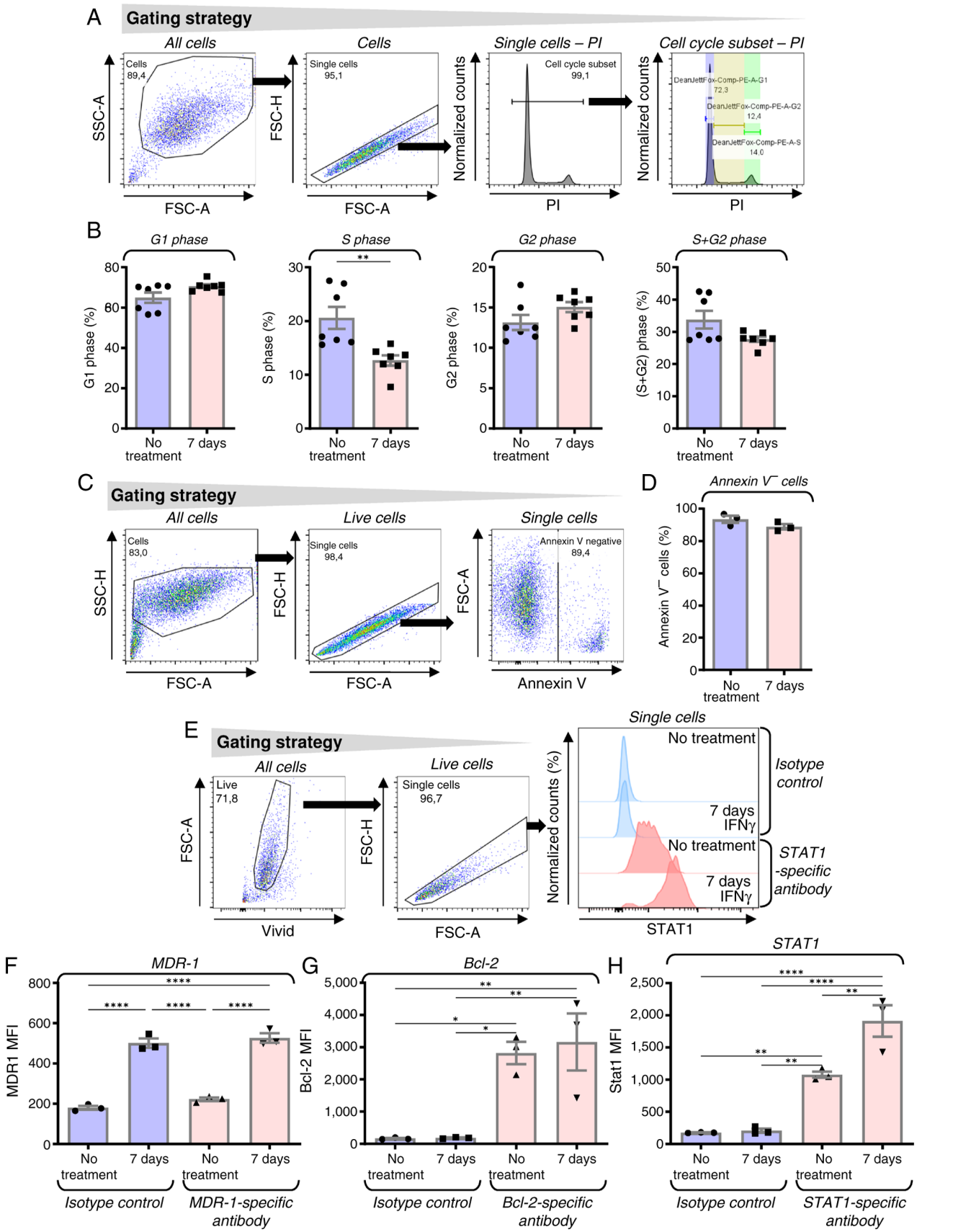

Figure 2. IFNγ in JBT19 cells changes the cell cycle, does not induce apoptosis and increases STAT1 expression without inducing the surface expression levels of MDR-1 or enhancing the expression levels of Bcl-2. (A) Gating strategy for cell cycle analysis by flow cytometry using propidium iodide staining. (B) Cell cycle evaluation in vehicle-treated (No treatment) or 7-day treated (7 d) JBT19 cells with IFNγ (200 ng/ml). The data indicate the proportions of JBT19 cells in the G_1, S, G_2 and S + G_2 phases. **P<0.01. n=7. (C) Gating strategy for annexin V analysis by flow cytometry. (D) Proportions of annexin V^- cells. (E) Gating strategy of flow cytometry data from intracellular staining. Staining with isotype controls or specific antibodies against (F) MDR-1 (extracellular staining), (G) Bcl-2 (intracellular staining) or (H) STAT1 (intracellular staining). The graphs demonstrate the evaluation of mean fluorescence intensity (MFI) staining. n=3 independent experiments. PD-L1, programmed cell death-ligand 1; MHC, major histocompatibility complex; nM, nanomolar.

Specifically, 5 days after 2-day IFNγ treatment, PD-L1 expression was considerably higher compared with that in cells treated for 2 days and nearly reached the levels observed in 7-day-treated cells (Fig. 3D). These results indicated that, after 2-day IFNγ treatment, the removal of the cytokine did not prevent the cells from further increasing the expression levels of PD-L1. These findings were also observed in the expression levels of MHC-I (Fig. 3D). However, the most notable finding was observed upon the evaluation of the surface expression levels of MHC-II: JBT19 cells that were negative or weakly positive for this molecule became positive after 2-day treatment with IFNγ and the levels were largely enhanced after 7-day treatment with IFNγ (Fig. 3D). Furthermore, the expression levels of MHC-II followed the same pattern as PD-L1 and MHC-I molecules; namely, the levels of MHC-II in cells cultured for 5 days after 2-day IFNγ treatment were markedly higher compared with the levels in 2-day-treated cells and nearly reached the levels of 7-day-treated cells. With an extended exposure to 14-day-treatment, the levels of MHC-II did not exhibit any further notable increase, which indicated that the IFNγ-elicited phenotypic changes were reaching their plateau within this length of treatment (Fig. 3E).

Onset of IFNγ-induced phenotypic remodeling and docetaxel resistance occurs shortly after exposure to IFNγ. IFNγ induces a signaling pathway that results in changes in the gene expression pattern within hours after the stimulation (52,55). Using the expression levels of MHC-II as a marker of the IFNγ-elicited phenotypic remodeling, it was identified that MHC-II expression was significantly enhanced after 24-h treatment with IFNγ (Fig. 3F). However, it was revealed that 6-h treatment with IFNγ enhanced their resistance to docetaxel by ~10-fold when IFNγ was subsequently removed during MTT assay (Fig. 3G and H). When IFNγ was present (not removed) during the subsequent 3-day MTT assay, their resistance to docetaxel increased ~100-fold (Fig. 3G and I). These findings indicated that the onset of JBT19-induced functionality changes (chemoresistance) occurred within hours after their exposure to IFNγ and continued to be enhanced with ongoing exposure.

IFNγ-induced phenotypic remodeling and docetaxel resistance is sustained for extended time but is reversible. The results in Fig. 3 indicated that the impact of IFNγ on JBT19 cells was sustained and possibly irreversible, potentially causing permanent changes in JBT19 cells. To investigate this, 7-day treated JBT19 cells were further cultured in the absence of IFNγ for 9 days (Fig. 4A, Rev0-9) and their proliferation rate was compared with that of cells cultured in the presence of IFNγ (Fig. 4A, IFNγ). Removal of IFNγ from the cells revealed a tendency to accelerate cell proliferation (Fig. 4B); the 9-day cell number fold increase accelerated from ~2- to 4-fold increase. Therefore, 9 days after cytokine removal, the cells were again passaged and cultured for subsequent 15 days and their proliferation rate (Fig. 4A, Rev9-24) was compared with that of IFNγ non-treated JBT19 cells (Fig. 4A, No treatment). The proliferation rates of the treated (Rev9-24) and control cells (No treatment) were comparable (Fig. 4C). To confirm that JBT19 cells regained the same proliferation rate after 24 days of culture without IFNγ, doubling times were determined for both treated (Fig. 4, Rev24) and control cells (Fig. 4, No treatment 2). The expansion of the previously treated JBT19 cells was now similar to that of their non-treated counterpart and both cell groups demonstrated comparable doubling times (Fig. 4D). Thus, the impact of IFNγ on cell proliferation was completely reversed 24 days after IFNγ removal.

Next, the present study investigated cell proliferation recovery also translated into the reversion of the cell surface markers PD-L1, MHC-I and MHC-II. As shown, the expression levels of PD-L1, MHC-I and MHC-II returned to the levels of the IFNγ non-treated cells (Fig. 4E).

To evaluate whether the extended cell culture-elicited reversion also translated into resensitization of the cells to docetaxel, the cells were analyzed by MTT assay. The previously treated JBT19 cells regained the same sensitivity to docetaxel as their non-treated counterparts (Fig. 4F). Collectively, these results demonstrated that the changes elicited by IFNγ were sustained but not permanent because the treated JBT19 cells could regain back the phenotypic and functional properties of the non-treated cells.

IFNγ-elicited chemoresistance is not JBT19 cell-restricted and can be mitigated by mitomycin C or doxorubicin in JBT19 cells. The JBT19 cell line was established from soft tissue sarcoma (28), which is a tumor of mesenchymal origin (59). To determine whether IFNγ induced docetaxel resistance in epithelial-derived tumors, the prostate carcinoma cell line PC-3 was utilized (29). Similar to JBT19 cells, 7-day IFNγ treatment induced resistance to docetaxel in PC-3 cells (Fig. 5A). indicating that the mechanism observed in JBT19 cells also takes place in cell lines of distinct histological origin.

Docetaxel is a chemotherapeutic agent that primarily targets rapidly dividing cells (60,61). The present study results indicated that IFNγ treatment markedly reduced the proliferation rate of JBT19 cells, suggesting that this decrease in proliferation could be the main mechanism underlying JBT19 cell resistance to docetaxel. To determine whether chemotherapeutics capable of targeting slowly dividing cells could overcome IFNγ-induced resistance, mitomycin C (62,63) and doxorubicin (64) were evaluated. The results revealed that both agents effectively targeted JBT19 cells at submicromolar concentrations (Fig. 5B and C) and that these agents were still effective against IFNγ-treated JBT19 cells, albeit their effective concentrations increased ~10-fold for mitomycin C and 6-fold for doxorubicin (Fig. 5B and C). Nevertheless, their performance was markedly improved compared with that of docetaxel, for which the effective concentration increased >2,000-fold following IFNγ treatment, as aforementioned. These results thus suggested that the IFNγ-elicited decrease in the proliferation of JBT19 cells could be the underlying mechanisms of the observed docetaxel resistance.

IFNγ treatment of JBT19 cells has no impact on in vitro antitumor adaptive immune response. The IFNγ-induced chemoresistance of JBT19 cells may limit the treatment options once similarly behaving cancer cells are present in tumors of the patients. To investigate whether IFNγ treatment could also limit the ability of the immune system to elicit a specific

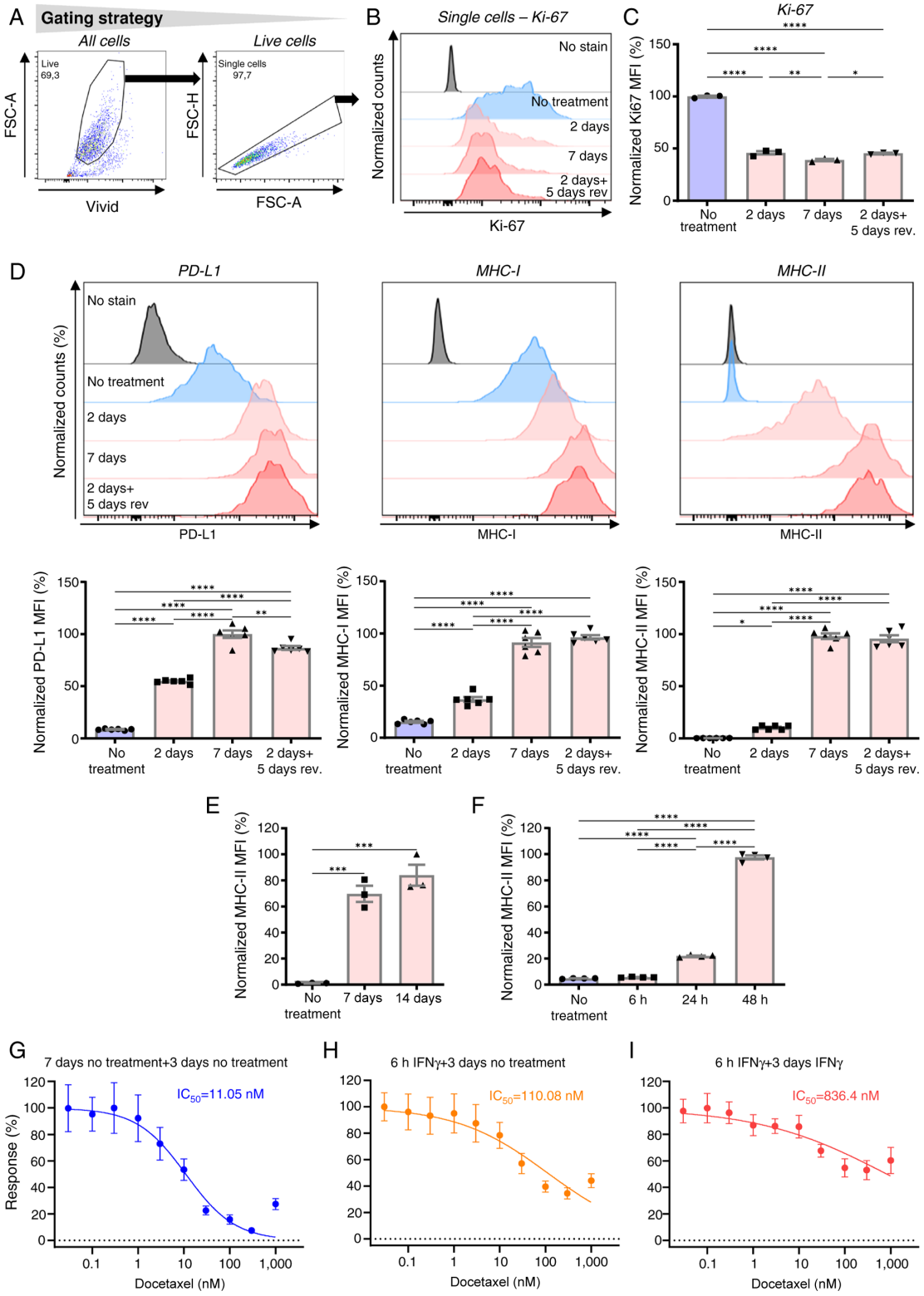

Figure 3. In JBT19 cells, IFNγ decreases the intracellular expression levels of Ki-67, increases the extracellular expression levels of PD-L1 and MHC-I and enhances the expression levels of MHC-II. (A) Gating strategy of flow cytometry data. (B) Intracellular staining with anti-Ki-67-specific antibody in vehicle-treated (No treatment), 2-day treated (2 d) or 7-day treated (7 d) JBT19 cells with IFNγ (200 ng/ml). Alternatively, the cells were treated for 2 days with IFNγ (200 ng/ml) and the cytokine was then extensively removed, while the cells were cultured in vehicle alone for additional 5 days (2d + 5d rev). As control (No stain) for individual fluorochromes, staining with vehicle alone was used. (C) Evaluation of the MFI staining in panel B. (D) Histograms of extracellular staining with anti-PD-L1-, MHC-I- or MHC-II-specific antibodies in samples treated as in panel B. The control (No stain) for individual fluorochromes was staining with vehicle alone. *P<0.05 and **P<0.01 and ****P<0.0001; C, n=3 (Ki-67) independent experiments. D, n=6. (E) Extracellular MHC-II staining of 14-day vehicle-treated (No treatment), 7-day or 14-day IFNγ-treated (IFNγ, 200 ng/ml) JBT19 cells. (F) Extracellular MHC-II staining of 48-h vehicle-treated or 6-, 24- or 48-h IFNγ-treated (IFNγ, 200 ng/ml) JBT19 cells. *P<0.05, **P<0.01, ***P<0.001 and ****P<0.0001; E, n=3 independent experiments. F, n=4 independent experiments. Panels E and F, one-way ANOVA with Tukey's post hoc test. MTT assay of (G) vehicle-treated JBT19 cells or (H and I) JBT19 cells treated for 6 h with IFNγ (200 ng/ml). Next, the treated JBT19 cells were rinsed and exposed to docetaxel at the indicated concentrations for 3 days in the (G and H) absence (no treatment + 3 d no treatment, 6 h IFNγ+3 d no treatment) or (I) presence of IFNγ (200 ng/ml). The calculated IC_{50} from n=3 independent experiments is shown. IFNγ, interferon γ; MFI, mean fluorescence intensity; d, days; PD-L1, programmed cell death-ligand 1; MHC, major histocompatibility complex; nM, nanomolar.

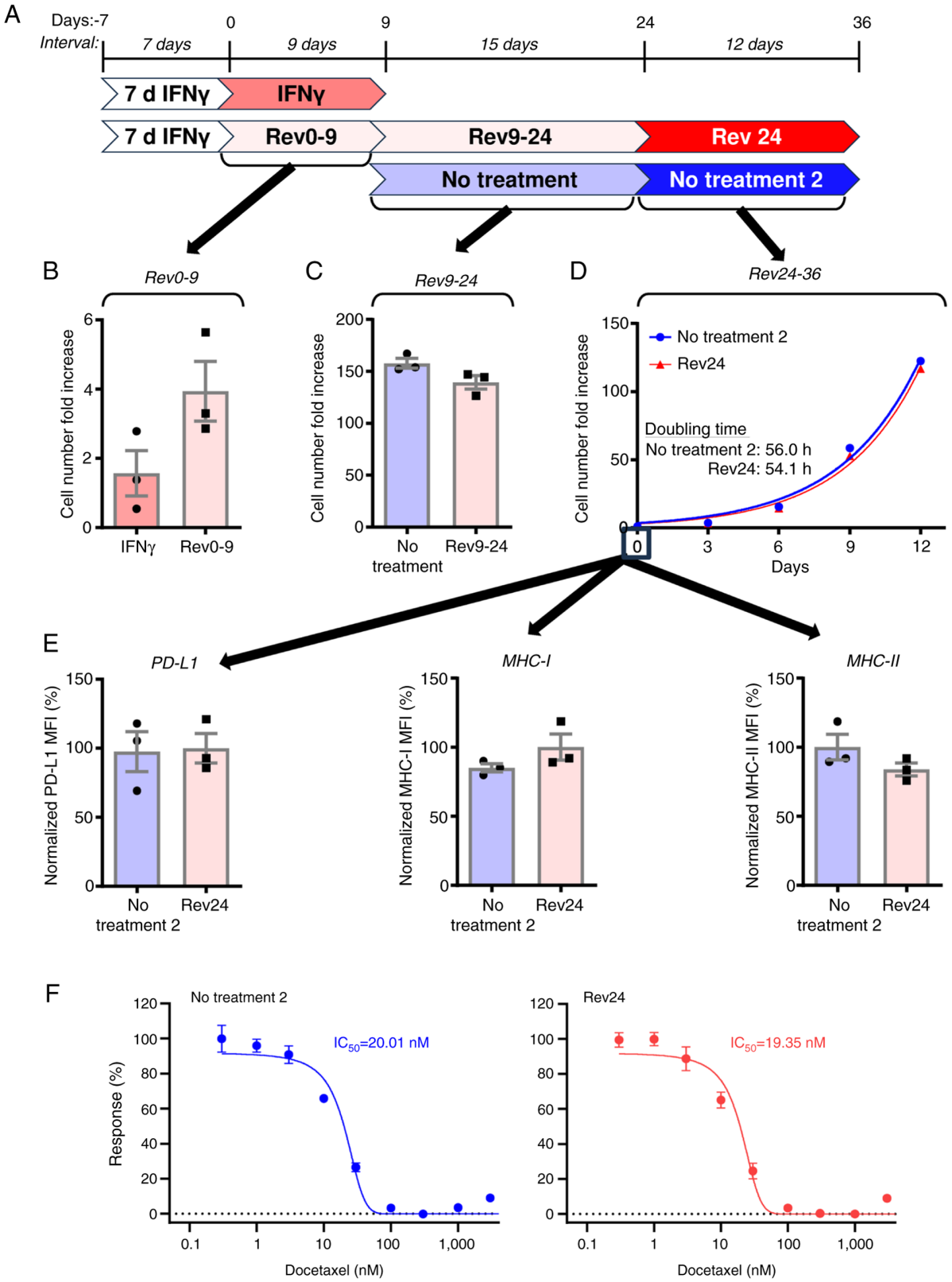

Figure 4. IFNγ-induced phenotypic remodeling and docetaxel resistance are sustained for an extended time but are reversible. (A) Schematic representation of the times of the experiment. (B) JBT19 cells were 7-day treated with IFNγ (200 ng/ml). The cells were then passaged and cultured for 9 days in the presence (IFNγ; dark pink) or absence (Rev0-9; No treatment, light pink) of IFNγ (200 ng/ml) and cell number fold increase was determined. (C) The Rev0-9 sample of JBT19 cells from panel B (Rev9-24, light pink) or JBT19 cells not treated with IFNγ (No treatment, light blue) were passaged and cultured in the absence of IFNγ for 15 days and the cell number fold increase was determined. (D) Rev9-24 sample of JBT19 cells from C (Rev24, light pink) and vehicle-treated sample of JBT19 cells from C (No treatment, light blue) were passaged and cultured for 12 days. Next, the cell number fold increase was determined at the indicated days and proliferation curves and pertinent doubling times were calculated. (E) Evaluation of the mean fluorescence intensities of extracellular staining with anti-PD-L1-, MHC-I- or MHC-II-specific antibodies in the Rev24 sample of JBT19 cells at day 0 from panel D (Rev24, light pink) and vehicle-treated sample of JBT19 cells at day 0 (No treatment 2, light blue). (F) Results of MTT assay of No treatment 2 (blue) and Rev24 (red) samples at day 0 from panel D. Cells were exposed to docetaxel at the indicated concentrations for 3 days. The calculated IC_{50} are shown (n=3 independent experiments). MFI, mean fluorescence intensity (arbitrary units); IFNγ, interferon γ; nM, nanomolar; PD-L1, programmed cell death-ligand 1; MHC, major histocompatibility complex.

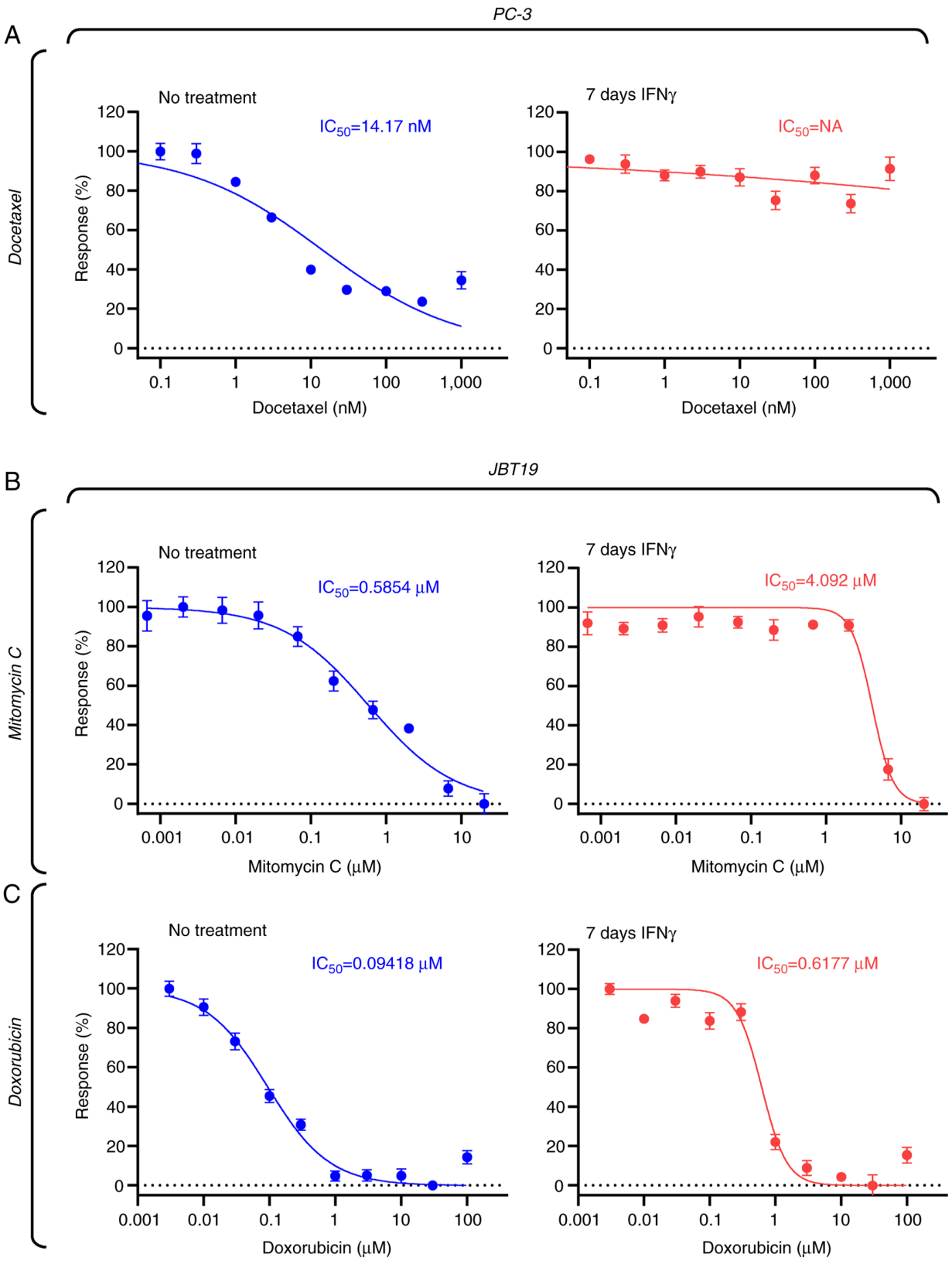

Figure 5. IFNγ-induced chemoresistance is not JBT19 cell-restricted and can be mitigated by mitomycin C or doxorubicin in JBT19 cells. (A) MTT assay of vehicle-treated (No treatment) or 7-day IFNγ-treated (IFNγ, 200 ng/ml) PC-3 cells exposed to docetaxel at the indicated concentrations for 3 days. MTT assay of vehicle-treated (No treatment) or 7-day IFNγ-treated (IFNγ, 200 ng/ml) JBT19 cells exposed to (B) mitomycin C or (C) doxorubicin at the indicated concentrations for 3 days. The calculated IC_{50} from three independent experiments are shown. IFNγ, interferon γ; NA, not available; nM, nanomolar.

adaptive immune response, JBT19-reactive lymphocytes were *in vitro* produced as described previously (28), using either non-treated JBT19 cells (JBT19-primed, to produce JBT19-reactive lymphocytes) or 7-day IFNγ-treated JBT19 cells (γJBT19-primed, to produce γJBT19-reactive lymphocytes) to stimulate and enrich cell cultures with reactive lymphocytes.

As shown in Fig. S1A and B, the enriched cell cultures were viable and the majority of cells were T cells exhibiting tendencies to increased frequencies of $CD4^+$ and $CD8^+$ populations in the γJBT19-primed cell cultures. The produced JBT19- or γJBT19-reactive lymphocytes were then stimulated with either JBT19 or γJBT19 cells and their reactivity was evaluated through the expression levels of IFNγ and TNFα in the treated lymphocytes, as determined by intracellular staining and flow cytometry analyses. As shown in Fig. 6, $CD8^+$ T cells of the produced JBT19-primed or γJBT19-primed lymphocytes reacted with both JBT19 or γJBT19 cells (Fig. 6A and C). Although there were no differences in the reactivity of $CD8^+$ T cells between JBT19-primed and γJBT19-primed cultures in high-responder donors, γJBT19-primed lymphocyte cultures demonstrated enhanced enrichment, with reactive $CD8^+$ T cells in the low-responder donors, indicating that IFNγ treatment of JBT19 cells promoted their potential to increase lymphocyte reactivity and cell culture enrichment with reactive $CD8^+$ T cells in low-responder donors, presumably through enhanced cell surface expression levels of MHC-I (Fig. 6C).

A significant effect of JBT19 cell treatment with IFNγ was identified for $CD4^+$ T cells. As shown in Fig. 6, $CD4^+$ T cells became stimulated only with γJBT19 cells and only significantly in the γJBT19-primed lymphocytes, while only a negligible stimulation was observed in JBT19-primed lymphocytes (Fig. 6A and B). These results demonstrated that IFNγ treatment of JBT19 cells had no negative impact on the *in vitro* stimulation of JBT19/γJBT19-reactive lymphocytes and that the IFNγ-induced *de novo* expression levels of MHC-II on the surface of JBT19 cells subsequently enriched the reactive lymphocytes with γJBT19-reactive $CD4^+$ T cells, thus providing evidence of the immune functionality of IFNγ-induced MHC-II on the surface of JBT19 cells.

IFNγ treatment of JBT19 cells does not prevent in vitro amplification of antitumor-elicited adaptive immune response. Effective antitumor immunity is dependent on its amplification through a large-scale cell number expansion of antitumor-reactive lymphocytes. To evaluate whether IFNγ treatment of JBT19 cells used for stimulation and enrichment with γJBT19-reactive lymphocytes could limit their later amplification, the *in vitro*-enriched γJBT19-reactive lymphocytes were large-scale expanded using a modified REP previously described for the expansion of virus antigen-specific lymphocytes (34). Using this protocol, JBT19- or γJBT19-primed cell cultures could be *in vitro* expanded with enriched JBT19/γJBT19-reactive lymphocytes by ~2,000-fold (Fig. S1C). The large-scale expanded cell cultures were viable and nearly exclusively contained T cells, including their $CD4^+$ and $CD8^+$ populations (Fig. S1D and E). Similar to the enriched cell cultures, the $CD8^+$ T cells of the expanded cell cultures contained a significant population of JBT19- or γJBT19-reactive cells (Fig. 7B). In addition, within the limited number of donors, the expanded cell cultures enriched through γJBT19 (γJBT19-primed) demonstrated a notable tendency to enhanced frequencies of the γJBT19-reactive population compared with the JBT19-primed cell cultures (Fig. 7B). By contrast, the frequencies of JBT19-reactive $CD8^+$ T cells varied between the donors, revealing two high responders and two low responders (Fig. 7B). Regardless, the results demonstrated that IFNγ treatment of JBT19 cells had no detrimental effects on the ability of cells to induce and amplify a targeted $CD8^+$ T cell-based immune response against these cells or their non-treated counterparts.

The reactivity pattern of $CD4^+$ T cells was similar to the pattern observed with the enriched cell cultures. $CD4^+$ T cells became stimulated only with γJBT19 cells and only significantly in the γJBT19-primed and expanded lymphocytes, while negligible stimulation was observed in the JBT19-primed and expanded lymphocytes (Fig. 7A). Collectively, these results indicated that treatment of JBT19 cells with IFNγ did not prevent adaptive immunity to elicit and amplify a specific $CD4^+$ and $CD8^+$ T cell-based adaptive immune response against treated JBT19 cells.

Next, the present study investigated whether MHC-T cell receptor interactions on expanded lymphocytes contributed to their activation. Using MHC-I and MHC-II blocking antibodies, a significant reduction was observed in T cell response for TNFα- and TNFα/IFNγ-producing $CD4^+$ T cells (Fig. 7C) and for IFNγ- and TNFα/IFNγ-producing $CD8^+$ T cells (Fig. 7D). A notable fraction of reactive T cells remained responsive despite the presence of blocking antibodies, suggesting either incomplete blockade or the involvement of bystander stimulation (65).

In vitro large-scale expanded JBT19-reactive lymphocytes are efficient in eliminating IFNγ-induced docetaxel-resistant JBT19 cells. The finding that IFNγ treatment of JBT19 cells did not translate into impaired adaptive immune response suggested that IFNγ-induced chemoresistance could be overcome by targeted adaptive immunity. To investigate whether this targeted adaptive immunity could also be effective in eliminating cancer cells, the present study evaluated whether the JBT19- or γJBT19-primed and large-scale expanded cell cultures with enriched JBT19/γJBT19-reactive lymphocytes could eliminate cultured JBT19 or γJBT19 cells. For this purpose, GFP-expressing JBT19 cells (JBT19-GFP) that the present study group had previously established were used (28). As shown in Fig. 8, regardless of whether JBT19- or γJBT19-primed and large-scale expanded cell cultures were used, both cell culture types were able to efficiently eliminate IFNγ-treated (γJBT19-GFP) and non-treated (JBT19-GFP) JBT19-GPF cells. Thus, these results revealed that, although IFNγ treatment produced docetaxel-resistant JBT19 cells, these docetaxel-resistant cells were not *in vitro* resistant to targeted adaptive immune response.

Discussion

The present study demonstrated a dual impact of IFNγ on the sensitivity of a UPS cell line, JBT19, to the widely used chemotherapeutic docetaxel and the ability of this cell line to *in vitro* elicit and amplify a targeted immune response. IFNγ-elicited changes in JBT19 cells were identified to be sustained but not permanent, since the cells were able to regain their original phenotype and behavior prior to treatment with IFNγ. However, reconstitution of this phenotype and behavior took >3 weeks, revealing that IFNγ markedly, yet still reversibly, change the propensity of cancer cells for extended periods of time and thus modulate their long-term behavior and resilience towards other therapeutic interventions.

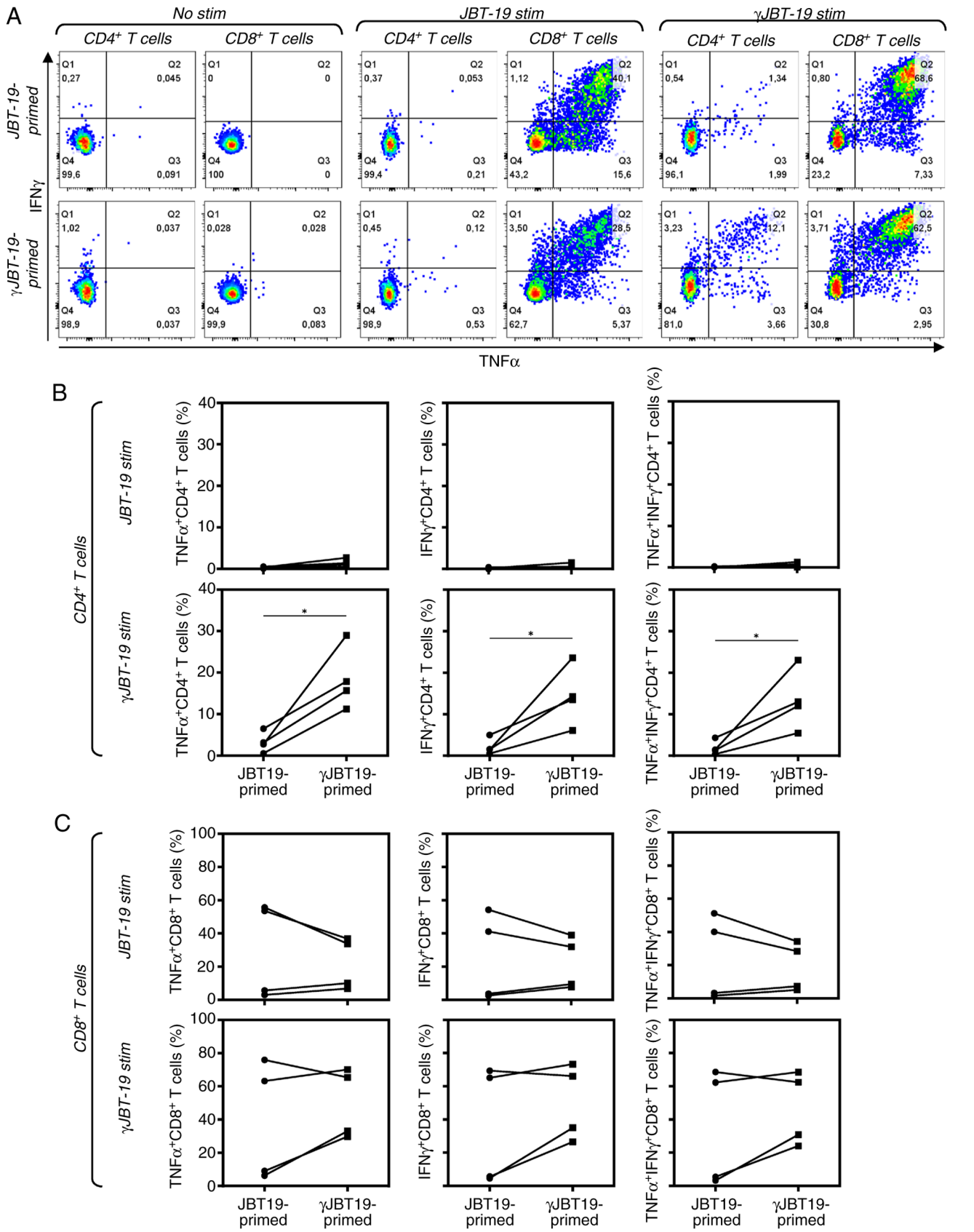

Figure 6. Reactivity of JBT19- or γJBT19 (7-day IFNγ-treated)-primed and enriched healthy donor lymphocytes to JBT19 or γJBT19 cells. (A) Lymphocytes of healthy donors were stimulated (primed) with non-treated (JBT19-primed) or 7-day IFNγ-treated (γJBT19-primed) JBT19 cells. The cell cultures were stimulated with vehicle alone (No stim), non-treated (JBT19-stim) or 7-day IFNγ-treated (γJBT19-stim) JBT19 cells and the lymphocyte reactivity was then determined by intracellular staining of IFNγ and TNFα and flow cytometry analysis. (B and C) The frequencies of TNFα- and/or IFNγ-producing $CD4^+$ or $CD8^+$ T cells in the gated $CD4^+$ or $CD8^+$ T cell ($CD3^+$) populations are shown. Evaluated frequencies of $TNF\alpha^+$-(left panels), $IFN\gamma^+$-(middle panels) and $TNF\alpha^+/IFN\gamma^+$-(right panels) producing JBT19- or γJBT19-primed and enriched healthy donors (B) $CD4^+$ or (C) $CD8^+$ T-cell populations after stimulation with non-treated (JBT19 stim) or 7-day IFNγ-treated (γJBT19-stim) JBT19 cells. In panels B and C, the statistically significant differences between JBT19- and γJBT19-primed cells were determined. $^*P<0.05$; n=4 healthy donors; paired two-tailed Student's t-test. IFNγ, interferon γ; stim, stimulation.

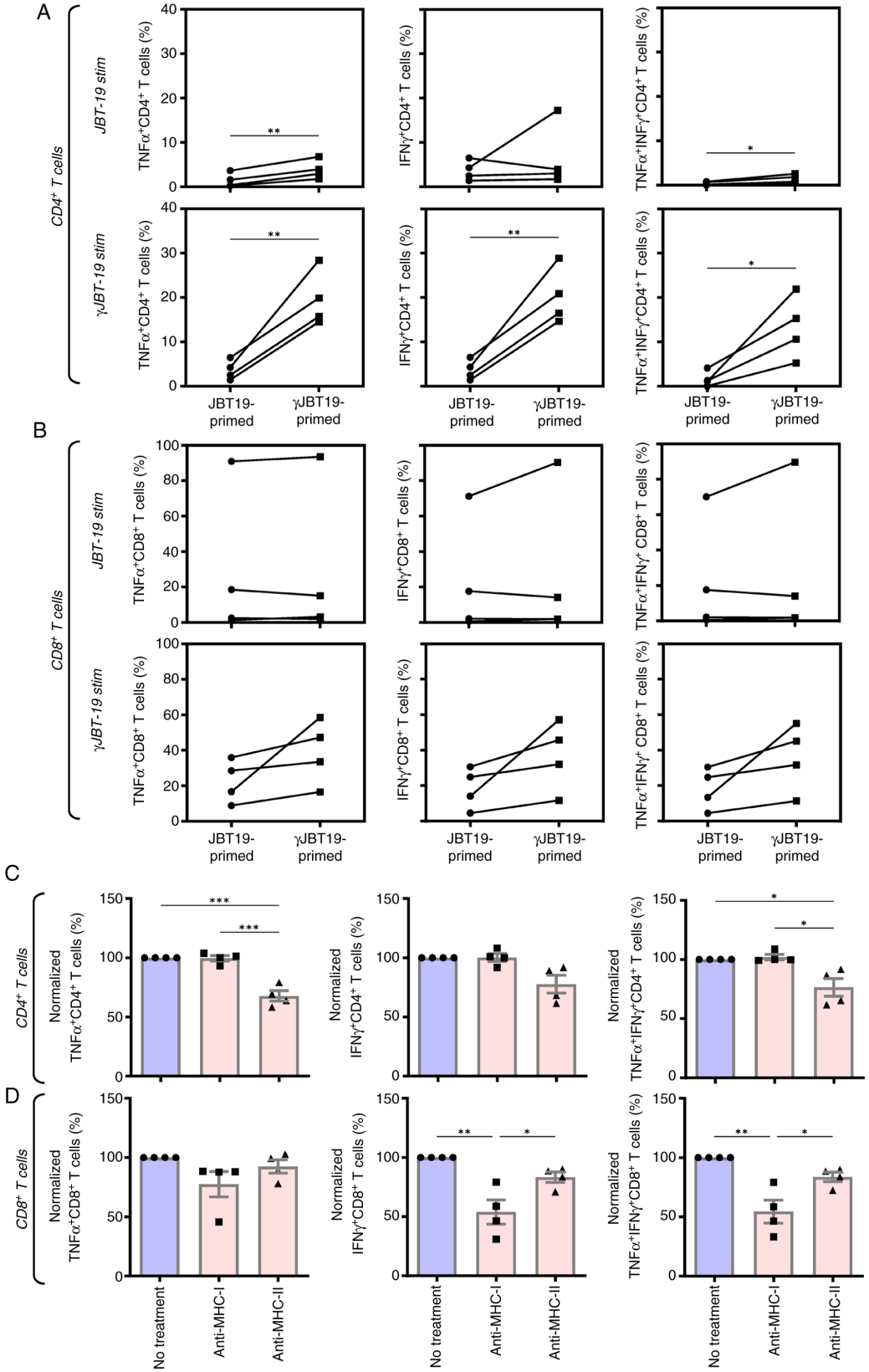

Figure 7. Reactivity of REP-expanded JBT19- or γJBT19 (7-day IFNγ-treated)-primed and enriched healthy donor lymphocytes to JBT19 or γJBT19 cells. (A) REP-expanded cell cultures were stimulated and lymphocyte reactivity was determined by intracellular staining of IFNγ and TNFα and flow cytometry analysis. The calculated frequencies of $TNF\alpha^+$-(left panels), $IFN\gamma^+$-(middle panels) and $TNF\alpha^+/IFN\gamma^+$-(right panels) producing JBT19- or γJBT19-primed and enriched healthy donors (B) $CD4^+$ or (C) $CD8^+$ T-cell populations in the REP-expanded cell cultures stimulated with non-treated (JBT19 stim) or 7-day IFNγ-treated (γJBT19-stim) JBT19 cells are shown. In panels A and B, the statistically significant differences between JBT19- and γJBT19-primed cells were determined ($^*P<0.05$, $^{**}P<0.01$; n=4 healthy donors; paired two-tailed Student's t-test). (C and D) The cells in panels A and B were pretreated or not for 30 min with 20 μg/ml anti-MHC-I or anti-MHC-II blocking antibodies in RPMI 1640 medium and then stimulated as shown in panels A and B in the presence or absence of 10 μg/ml blocking antibodies. Data are presented as means ± SEM. The statistically significant differences between the treatment groups are indicated ($^*P<0.05$, $^{**}P<0.01$ and $^{***}P<0.001$; n=3 independent experiments; one-way ANOVA with Tukey's post hoc test). IFNγ, interferon γ; REP, rapid expansion protocol; MHC, major histocompatibility complex.

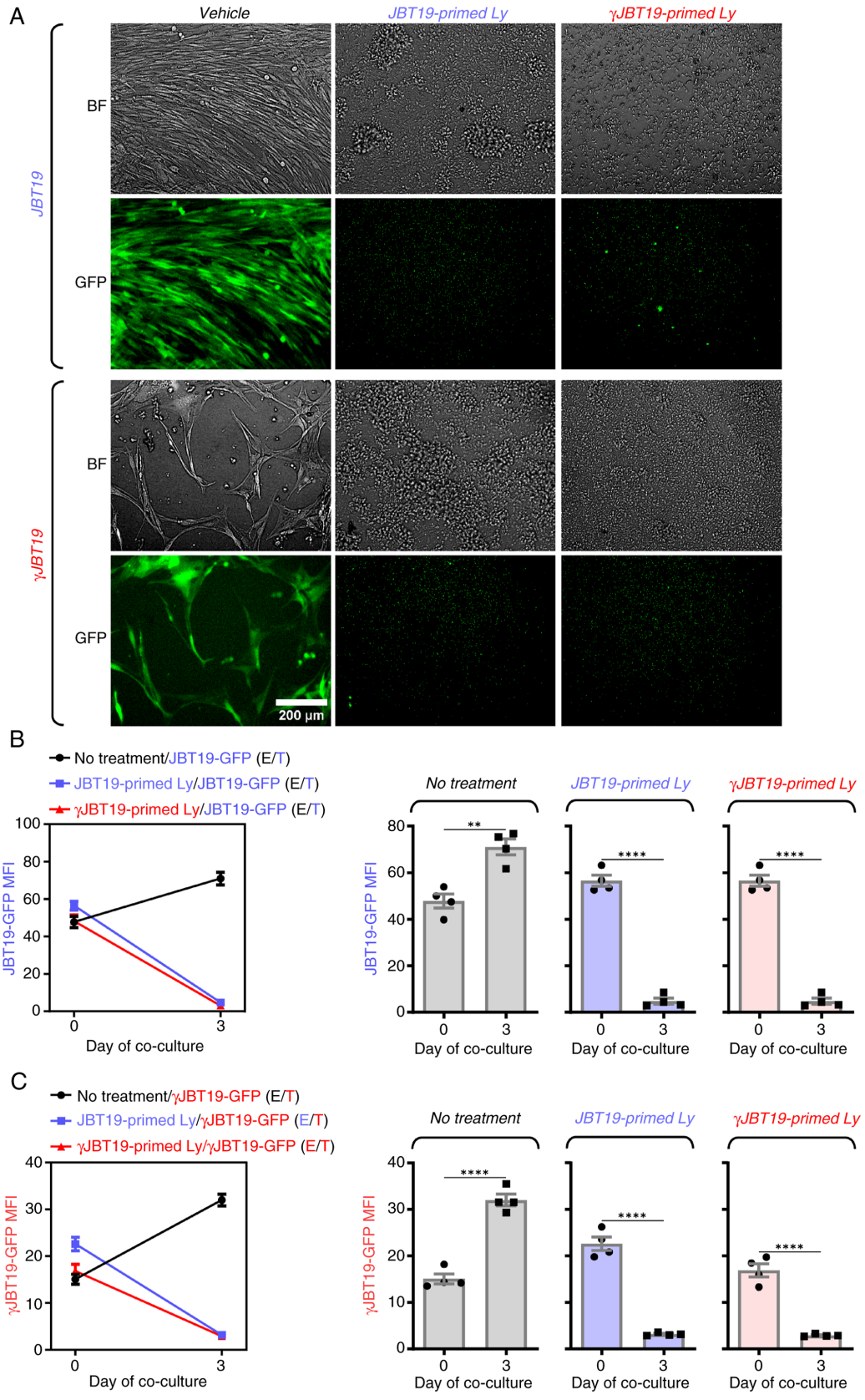

Figure 8. Cytotoxic impact of REP-expanded JBT19- or γJBT19 (7-day IFNγ-treated)-primed and enriched healthy donor lymphocytes on JBT19 and γJBT19 cells. (A) REP-expanded JBT19-(JBT19-primed Ly) or γJBT19-(γJBT19-primed Ly) primed and enriched healthy donor lymphocytes were cocultured with adherent non-treated (JBT19-GFP) or 7-day IFNγ-treated (γJBT19-GFP) JBT19-GFP cells for 3 days and images of BF and GFP fluorescence were acquired using a fluorescence microscope at 10 X magnification. (scale bar, 200 μm). JBT19-GFP or γJBT19-GFP cells cultured without lymphocytes were used as a positive control (No treatment). (B) The cytotoxic impact of the coculture on JBT19-GFP cells was evaluated via the MFI of GFP fluorescence (JBT19-GFP MFI) in the cell coculture, as described in the Materials and methods section. (C) Cytotoxic impact of the coculture on γJBT19-GFP cells was evaluated via the MFI of GFP fluorescence (γJBT19-GFP MFI) in the cell coculture. **P<0.01, ****P<0.0001; n=4 healthy donors; paired two-tailed Student's t-test). E; effector cells; T; target cells; IFNγ, interferon γ; MFI, mean fluorescence intensity; REP, rapid expansion protocol; BF, bright field; GFP, green fluorescent protein; Ly, lymphocytes.

The tumor microenvironment serves a key role in determining the behavior of the tumor and its resilience to elimination by multiple therapeutic approaches, including immunotherapy and chemotherapy (66,67). The long-term (chronic) effects of this microenvironment on immune, stromal and cancer cells can differ notably from short-term (acute) effects, which may affect mast cell and T cell stimulation as well as tumor cell metabolism (30,68-73). Any intervention targeting the tumor microenvironment can alter tumor behavior. Such changes may either make the tumor more sensitive to therapy or cause it to develop resistance (74-76). IFNγ is a cytokine that is a key component of the cell-mediated response to cancer cells (13,15,77). The present study confirmed its large production by the *in vitro*-produced JBT19-reactive $CD8^+$ T cells once these cells were exposed to JBT19 cells. Therefore, under immune attack, cancer cells are likely to be first exposed to this cytokine before they become eliminated by reactive cytotoxic lymphocytes. Using the cell line JBT19 as a model, the present study demonstrated that this exposure could markedly change the propensity of cancer cells under a presumable immune attack. IFNγ-exposed JBT19 cells nearly stopped proliferating and started to express multiple molecules that are associated with worse disease prognosis, immunoresistance, metastatic behavior, cancer cell stemness and cancer development [namely, CD44 (78), CD47 (41,79), PD-L1 (80-82) and CD95 (Fas) (43,83,84)]. However, one of the expressed molecules triggered by IFNγ in JBT19 cells could have an ambiguous functional role towards antitumor immunity: MHC-II. The expression levels of MHC-II are largely associated with professional antigen-presenting cells, where it is responsible for the stimulation of $CD4^+$ T cells. However, this molecule can also be expressed in other cell types such as tumor-associated fibroblasts or cancer cells (85). The cancer cell expression levels of MHC-II in murine tumor models is mostly associated with slower tumor growth, improved tumor rejection and increased tumor infiltration with immune cells (86,87). Furthermore, previous studies reported that MHC-II expression in tumor cells was associated with improved disease prognosis and response to immunotherapy, including immune checkpoint inhibitors (ICIs) (88-91). However, MHC-II expression in cancer cells can also drive resistance to immunotherapy (92), which can promote cancer cell metastasis (93). Using an IFNγ-JBT19-based study system, the present study findings could recapitulate and explain several of these contrasting findings associated with the expression levels of MHC-II in cancer cells. The expression levels of MHC-II in JBT19 cells were a consequence of long-term exposure to IFNγ, which also caused a notable decrease in the speed of proliferation of JBT19 cells. Furthermore, *in vitro*-enriched and -expanded JBT19-reactive lymphocytes produced IFNγ after their stimulation with JBT19 cells. Therefore, a close-by antitumor activity *in vivo* upon which cytotoxic lymphocytes attack cancer cells could be the source of IFNγ, which may induce MHC-II expression in the not-yet attacked cancer cells. As such, the expression levels of MHC-II in cancer cells could be thus viewed as a marker sensing ongoing antitumor immune activity in the vicinity of cancer cells. There, it could be considered that the expression levels of MHC-II in cancer cells of tumors could serve as a surrogate predictive marker for the efficacy of ICIs (anti-PD-1, anti-PDL-1), as this efficacy is increased in inflamed tumors (94). Similar conclusions could be inferred from the expression levels of PD-L1 in IFNγ-treated JBT19 cells, the expression levels of which are often enhanced in inflamed tumors, where IFNγ could be present at high levels in the tumor milieu, regulating, alongside other cytokines (IL-27, IL-1α) (95), the expression levels of PD-L1 in cancer cells (96). However, whether other cytokines in the tumor milieu could promote PD-L1 or MHC-II expression in JBT19 cells, remains to be further investigated in follow-up *in vivo* models using JBT19 cells and pertinent therapeutic interventions in the future.

Antitumor immune activity is key to tumor elimination. This activity is boosted or elicited by immunotherapy. As immunotherapy has become the first-line treatment in numerous oncological diagnoses, such as advanced non-small cell lung and advanced head and neck cancer or metastatic melanoma (3-6), antitumor immunity serves a key role in therapy-naïve tumors and changes their behavior, which can cause cancer cell immune evasion and resistance to immunotherapy (92,97,98). Although the present study indicated that IFNγ-treated JBT19 cells were *in vitro* efficiently eliminated by JBT19- or γJBT19-reactive lymphocytes, this scenario may not hold *in vivo*, where not all cancer cells often become readily and entirely eliminated (99). These cells may migrate to distant locations away from the tumor and exhibit their IFNγ-induced characteristics. One possible interaction could involve novel expression levels of MHC-II, which in turn may lead to the activation of regulatory $CD4^+$ T cells in lymph nodes (93). The present study demonstrated that γJBT19 cells *in vitro* induced the enrichment and expansion of γJBT19-reactive $CD4^+$ T cells, the reactivity of which was presumably dependent on the expression and functionality of MHC-II, since no enrichment or expansion of γJBT19-reactive $CD4^+$ T cells was observed in IFNγ non-treated JBT19 cells. However, whether these γJBT19-reactive $CD4^+$ T cells hold or could later acquire (92) a regulatory potential remains to be further elucidated. Nevertheless, the IFNγ-induced reversible but sustained reprogramming of cancer cells not only indicates the cancer cell plasticity that can be responsible for the disease resistance to immunotherapy and possible promotion of metastatic behavior (100-102), but may also have notable implications for other therapeutic modalities, including cytotoxic chemotherapy.

The robustness of the novel IFNγ-JBT19-based system helped demonstrate the marked impact of IFNγ on the proliferation of JBT19 cells and their expansion in cell culture. IFNγ treatment not only nearly stopped the expansion of JBT19 cells in the cell culture, but also made them resistant to the chemotherapeutic agent docetaxel, which is one of the widely used anticancer drugs (45). Immunotherapy that elicits or promotes an immune attack on tumors may indicate a therapeutic impact leading to the elimination of cancer cells; by contrast, it can also produce cancer cell immunoresistance. Therefore, although IFNγ is often considered a marker of effective immunotherapy, promoting both immune and cancer cells by increasing antigen presentation and recruiting more cancer cell-targeting immune cells to tumors, it can also exhibit the opposite role in the responses of patients to immunotherapy by contributing to the development of mechanisms associated with the acquisition of resistance to immunotherapy, including resistance to

ICIs (72,103). To the best of our knowledge, the present study is, however, the first to demonstrate that IFNγ can elicit resistance beyond immunotherapy, impacting chemotherapy.

The present study indicated that chronic exposure of JBT19 cells to IFNγ significantly slowed down their proliferation. This suggested that the cell line could become resistant to chemotherapeutics effective against dividing cells such as docetaxel (46). The choice to study docetaxel confirmed this expectation, as an increased resistance to the drug was observed. However, the extent of this acquired resistance was unexpected; a cell line that was initially sensitive to nM concentrations of the drug became nearly resistant to this drug after prolonged exposure to IFNγ. A similar observation was made in PC-3 cells, suggesting that this mechanism of resistance is not limited to sarcomas but may also be relevant in carcinoma cell lines (59). This finding contrasted with previous research, which demonstrated that IFNγ sensitized cancer cells to chemotherapy in a model of metastatic castration-resistant prostate cancer (104). However, this sensitization was based on 40-fold lower concentrations of IFNγ, 5 ng/ml vs. 200 ng/ml in the present study and only 2-day treatment vs. 7-day treatment. Furthermore, the cytotoxic effect was investigated in a combination with recombinant human TNF-related apoptosis inducing ligand (TRAIL), a molecule that serves a key role in the ability of the immune system to selectively induce apoptosis (programmed cell death) in cancer cells (105). TRAIL receptor expression or functionality is enhanced by IFNγ, which associates this modulation to both chemoresistance and immunoresistance (106,107). Therefore, the conditions of the present study were more robust concerning the IFNγ concentration and exposure time, absence of the contributing TRAIL ligand/TRAIL receptor-mediated cytotoxicity and presumably were more closely mimicking *in vivo* conditions under which local concentrations of IFNγ at sites of an ongoing and concentrated attack on cancer cells by cytotoxic lymphocytes could be increasing and the exposure time could be chronic.

Analysis of chemotherapeutics that target non-dividing or slowly dividing cells via multiple mechanisms, such as mitomycin C (108,109) and doxorubicin (110,111), further supports the notion that downregulation of cell proliferation could be a key mechanism underlying IFNγ-induced resistance. One potential driver of this mechanism is the observed upregulation of STAT1 in IFNγ-treated JBT19 cells. Upregulation of STAT1 has been associated not only with chemoresistance, including resistance to docetaxel (112,113), but also to mechanisms that can be mitigated by targeting the STAT signaling pathway (114,115). The detailed mechanism that underpins this drug resistance acquisition warrants further investigation, as well as its existence in other cell lines, its performance in 3D-culture/co-culture models or *in vivo* animal models and its potential interaction with other chemotherapeutics, particularly those whose cytotoxic impact is not as much cell proliferation-dependent, such as alkylating drugs, proteasome inhibitors and autophagy inhibitors (116,117). Conducting these validation studies will be key to determine the extent to which immune mechanisms drive drug resistance. Regardless of the scope of this mechanism that needs to be addressed in follow-up studies, the use of JBT19 cells in the present study enabled to describe a novel IFNγ-driven mechanism that provides evidence of the interplay between immunotherapy and cancer cell chemoresistance.

This novel mechanism could have notable implications for immunotherapy and other treatment options (targeted therapy) where IFNγ signatures can serve a notable role (118). IFNγ signatures are frequently associated with improved responses to immunotherapy (20,21,72,119). However, these responses are often insufficient to fully prevent disease progression. After immunotherapy failure, chemotherapy commonly remains a standard treatment option (120,121). In certain cases, the chemotherapy outcome is greater than expected in the absence of prior immunotherapy (22,23). In certain instances, chemotherapy efficacy is not improved (122). However, there are also studies indicating that chemotherapy can be less effective following failed immunotherapy compared with treatment-naïve conditions (24,25).

The present study revealed a novel mechanism that may underline the immunotherapy-induced acquisition of transient chemotherapy resistance, which could be associated with enhanced IFNγ signatures often associated with immunotherapy (20,21,72,119). The present study demonstrated that this IFNγ-mediated resistance differentially impacted chemotherapeutic agents, rendering cancer cells either completely resistant to certain drugs (such as docetaxel) or partially resistant to others (such as mitomycin C and doxorubicin). From a clinical perspective, these findings suggested that therapeutic decision-making after immunotherapy failure should account for this mechanism when selecting subsequent chemotherapeutic regimens. Furthermore, similar considerations should be applied during the design of next-generation therapeutics, such as antibody-drug conjugates or nanoparticle-drug conjugates, particularly when choosing the chemotherapeutic payloads to maximize efficacy (123).

The present study reported a robust system based on a novel UPS cell line, JBT19, through which a dual identity of IFNγ towards chemoresistance and immunostimulation was demonstrated *in vitro*. This dual identity materialized through sustained but reversible phenotypical and functional changes in IFNγ-impacted JBT19 cells, and produced chemoresistance on one side, and enhanced immunostimulatory potential on the other. Although this dual identity could be cell line- and condition-specific, its engagement under specific disease conditions and therapy could markedly affect the outcome of therapy. Therefore, these findings could have potentially notable implications for combined therapies, namely for the combinations of immunotherapy and chemotherapy in the future.

In conclusion, to the best of our knowledge, the present study revealed for the first time the 'dual role' in chronic IFNγ exposure, leading to both chemoresistance and immunosensitivity. This may have key implications for the interplay between the effectiveness of cytotoxic chemotherapy and immunotherapy.

Acknowledgements

Not applicable.

Funding

The present study was supported by the Ministry of Health, Czech Republic (grant no. NU23-08-00071).

Availability of data and materials

The data generated in the present study may be requested from the corresponding author.

Authors' contributions

PT and DSt performed cell culture, viability and flow cytometry analyses. DSt performed cytotoxic analyses. PT and DSm conceived and designed the present study. DSm supervised the present study. DSt contributed to the present study design. DSm wrote the manuscript. PT and DSt wrote the manuscript and confirm the authenticity of all the raw data. All authors read and approved the final manuscript.

Ethics approval and consent to participate

All experimental protocols were approved by the ethics standards of the institutional, national research committee (Ethics Committee of the University Hospital Motol in Prague; approval no. EK-602.4/22; Prague, Czech Republic). All experiments were performed in accordance with the 1964 Declaration of Helsinki and its later amendments or comparable ethics standards. All volunteers included in the present study signed an informed consent form for the use of their blood-derived products in future research.

Patient consent for publication

Not applicable.

Competing interests

The authors declare that they have no competing interests.

References

1. Sun H, Liu J, Hu F, Xu M, Leng A, Jiang F and Chen K: Current research and management of undifferentiated pleomorphic sarcoma/myofibrosarcoma. Front Genet 14: 1109491, 2023.
2. Wu JT, Nowak E, Imamura J, Leng J, Shepard D, Campbell SR, Scott J, Nystrom L, Mesko N, Schwartz GK and Burke ZDC: Immunotherapy in the treatment of undifferentiated pleomorphic sarcoma and myxofibrosarcoma. Curr Treat Options Oncol 26: 891-909, 2025.
3. Wang J and Wu L: First-line immunotherapy for advanced non-small cell lung cancer: Current progress and future prospects. Cancer Biol Med 21: 117-124, 2023.
4. Reardon S: First cell therapy for solid tumours heads to the clinic: What it means for cancer treatment. Nature: Mar 11, 2024 doi: 10.1038/d41586-024-00673-w (Epub ahead of print).
5. Huang Y, Zhou H, Zhao G, Wang M, Luo J and Liu J: Immune checkpoint inhibitors serve as the First-line treatment for advanced head and neck cancer. Laryngoscope 134: 749-761, 2024.
6. Lamba N, Ott PA and Iorgulescu JB: Use of First-line immune checkpoint inhibitors and association with overall survival among patients with metastatic melanoma in the Anti-PD-1 Era. JAMA Netw Open 5: e2225459, 2022.
7. Yau T, Galle PR, Decaens T, Sangro B, Qin S, da Fonseca LG, Karachiwala H, Blanc JF, Park JW, Gane E, *et al*: Nivolumab plus ipilimumab versus lenvatinib or sorafenib as first-line treatment for unresectable hepatocellular carcinoma (CheckMate 9DW): An Open-label, randomised, phase 3 trial. Lancet 405: 1851-1864, 2025.
8. Diker O and Olgun P: Salvage chemotherapy in patients with nonsmall cell lung cancer after prior immunotherapy: Aa retrospective, real-life experience study. Anticancer Drugs 33: 752-757, 2022.
9. Assi HI, Zerdan MB, Hodroj M, Khoury M, Naji NS, Amhaz G, Zeidane RA and El Karak F: Value of chemotherapy post immunotherapy in stage IV non-small cell lung cancer (NSCLC). Oncotarget 14: 517-525, 2023.
10. Sordo-Bahamonde C, Lorenzo-Herrero S, Gonzalez-Rodriguez AP, Martínez-Pérez A, Rodrigo JP, García-Pedrero JM and Gonzalez S: Chemo-immunotherapy: A new trend in cancer treatment. Cancers (Basel) 15: 2912, 2023.
11. Zhang Z, Liu X, Chen D and Yu J: Radiotherapy combined with immunotherapy: The dawn of cancer treatment. Signal Transduct Target Ther 7: 258, 2022.
12. Ni L and Lu J: Interferon gamma in cancer immunotherapy. Cancer Med 7: 4509-4516, 2018.
13. Castro F, Cardoso AP, Goncalves RM, Serre K and Oliveira MJ: Interferon-gamma at the crossroads of tumor immune surveillance or evasion. Front Immunol 9: 847, 2018.
14. Martinez-Lostao L, Anel A and Pardo J: How do cytotoxic lymphocytes kill cancer cells? Clin Cancer Res 21: 5047-5056, 2015.
15. Bhat P, Leggatt G, Waterhouse N and Frazer IH: Interferon-γ derived from cytotoxic lymphocytes directly enhances their motility and cytotoxicity. Cell Death Dis 8: e2836, 2017.
16. Mazet JM, Mahale JN, Tong O, Watson RA, Lechuga-Vieco AV, Pirgova G, Lau VWC, Attar M, Koneva LA, Sansom SN, *et al*: IFNgamma signaling in cytotoxic T cells restricts anti-tumor responses by inhibiting the maintenance and diversity of intra-tumoral stem-like T cells. Nat Commun 14: 321, 2023.
17. Jorgovanovic D, Song M, Wang L and Zhang Y: Roles of IFN-γ in tumor progression and regression: A review. Biomark Res 8: 49, 2020.
18. Jing ZL, Liu GL, Zhou N, Xu DY, Feng N, Lei Y, Ma LL, Tang MS, Tong GH, Tang N and Deng YJ: Interferon-γ in the tumor microenvironment promotes the expression of B7H4 in colorectal cancer cells, thereby inhibiting cytotoxic T cells. Sci Rep 14: 6053, 2024.
19. Abiko K, Matsumura N, Hamanishi J, Horikawa N, Murakami R, Yamaguchi K, Yoshioka Y, Baba T, Konishi I and Mandai M: IFN-γ from lymphocytes induces PD-L1 expression and promotes progression of ovarian cancer. Br J Cancer 112: 1501-1509, 2015.
20. Wong CW, Huang YY and Hurlstone A: The role of IFN-γ-signalling in response to immune checkpoint blockade therapy. Essays Biochem 67: 991-1002, 2023.
21. Reijers ILM, Rao D, Versluis JM, Menzies AM, Dimitriadis P, Wouters MW, Spillane AJ, Klop WMC, Broeks A, Bosch LJW, *et al*: IFN-γ signature enables selection of neoadjuvant treatment in patients with stage III melanoma. J Exp Med 220: e20221952, 2023.
22. Casadei B, Argnani L, Morigi A, Lolli G, Broccoli A, Pellegrini C, Nanni L, Stefoni V, Coppola PE, Carella M, *et al*: Effectiveness of chemotherapy after anti-PD-1 blockade failure for relapsed and refractory Hodgkin lymphoma. Cancer Med 9: 7830-7836, 2020.
23. Saleh K, Daste A, Martin N, Pons-Tostivint E, Auperin A, Herrera-Gomez RG, Baste-Rotllan N, Bidault F, Guigay J, Le Tourneau C, *et al*: Response to salvage chemotherapy after progression on immune checkpoint inhibitors in patients with recurrent and/or metastatic squamous cell carcinoma of the head and neck. Eur J Cancer 121: 123-129, 2019.
24. Goldinger SM, Buder-Bakhaya K, Lo SN, Forschner A, McKean M, Zimmer L, Khoo C, Dummer R, Eroglu Z, Buchbinder EI, *et al*: Chemotherapy after immune checkpoint inhibitor failure in metastatic melanoma: A retrospective multicentre analysis. Eur J Cancer 162: 22-33, 2022.
25. Black M, Barsoum IB, Truesdell P, Cotechini T, Macdonald-Goodfellow SK, Petroff M, Siemens DR, Koti M, Craig AW and Graham CH: Activation of the PD-1/PD-L1 immune checkpoint confers tumor cell chemoresistance associated with increased metastasis. Oncotarget 7: 10557-10567, 2016.
26. Lazcano R, Barreto CM, Salazar R, Carapeto F, Traweek RS, Leung CH, Gite S, Mehta J, Ingram DR, Wani KM, *et al*: The immune landscape of undifferentiated pleomorphic sarcoma. Front Oncol 12: 1008484, 2022.
27. Wei X, Ruan H, Zhang Y, Qin T, Zhang Y, Qin Y and Li W: Pan-cancer analysis of IFN-gamma with possible immunotherapeutic significance: A verification of single-cell sequencing and bulk omics research. Front Immunol 14: 1202150, 2023.
28. Taborska P, Lukac P, Stakheev D, Rajsiglova L, Kalkusova K, Strnadova K, Lacina L, Dvorankova B, Novotny J, Kolar M, *et al*: Novel PD-L1- and collagen-expressing patient-derived cell line of undifferentiated pleomorphic sarcoma (JBT19) as a model for cancer immunotherapy. Sci Rep 13: 19079, 2023.

29. Kaighn ME, Narayan KS, Ohnuki Y, Lechner JF and Jones LW: Establishment and characterization of a human prostatic carcinoma cell line (PC-3). Invest Urol 17: 16-23, 1979.
30. Taborska P, Stakheev D, Svobodova H, Strizova Z, Bartunkova J and Smrz D: Acute conditioning of Antigen-expanded CD8+ T cells via the GSK3β-mTORC axis differentially dictates their immediate and distal responses after antigen rechallenge. Cancers (Basel) 12: 3766, 2020.
31. Smrž D, Kim MS, Zhang S, Mock BA, Smrzová S, DuBois W, Simakova O, Maric I, Wilson TM, Metcalfe DD and Gilfillan AM: mTORC1 and mTORC2 differentially regulate homeostasis of neoplastic and non-neoplastic human mast cells. Blood 118: 6803-6813, 2011.
32. Smrž D, Dráberová L and Dráber P: Non-apoptotic phosphatidylserine externalization induced by engagement of glycosylphosphatidylinositol-anchored proteins. J Biol Chem 282: 10487-10497, 2007.
33. Taborska P, Bartunkova J and Smrz D: Simultaneous in vitro generation of human CD34+-derived dendritic cells and mast cells from non-mobilized peripheral blood mononuclear cells. J Immunol Methods 458: 63-73, 2018.
34. Taborska P, Lastovicka J, Stakheev D, Strizova Z, Bartunkova J and Smrz D: SARS-CoV-2 spike glycoprotein-reactive T cells can be readily expanded from COVID-19 vaccinated donors. Immun Inflamm Dis 9: 1452-1467, 2021.
35. Stakheev D, Taborska P, Kalkusova K, Bartunkova J and Smrz D: LL-37 as a powerful molecular tool for boosting the performance of ex vivo-Produced human dendritic cells for cancer immunotherapy. Pharmaceutics 14: 2747, 2022.
36. Stakheev D, Taborska P, Strizova Z, Podrazil M, Bartunkova J and Smrz D: The WNT/β-catenin signaling inhibitor XAV939 enhances the elimination of LNCaP and PC-3 prostate cancer cells by prostate cancer patient lymphocytes in vitro. Sci Rep 9: 4761, 2019.
37. Molgora M, Cortez VS and Colonna M: Killing the invaders: NK cell impact in tumors and Anti-tumor therapy. Cancers (Basel) 13: 595, 2021.
38. Zhang S, Liu W, Hu B, Wang P, Lv X, Chen S and Shao Z: Prognostic significance of Tumor-infiltrating natural killer cells in solid tumors: A systematic review and Meta-analysis. Front Immunol 11: 1242, 2020.
39. Sun YP, Ke YL and Li X: Prognostic value of CD8+ tumor-infiltrating T cells in patients with breast cancer: A systematic review and meta-analysis. Oncol Lett 25: 39, 2023.
40. Yaghobi Z, Movassaghpour A, Talebi M, Abdoli Shadbad M, Hajiasgharzadeh K, Pourvahdani S and Baradaran B: The role of CD44 in cancer chemoresistance: A concise review. Eur J Pharmacol 903: 174147, 2021.
41. Wang H, Tan M, Zhang S, Li X, Gao J, Zhang D, Hao Y, Gao S, Liu J and Lin B: Expression and significance of CD44, CD47 and c-met in ovarian clear cell carcinoma. Int J Mol Sci 16: 3391-3404, 2015.
42. Yoshida K, Tsujimoto H, Matsumura K, Kinoshita M, Takahata R, Matsumoto Y, Hiraki S, Ono S, Seki S, Yamamoto J and Hase K: CD47 is an adverse prognostic factor and a therapeutic target in gastric cancer. Cancer Med 4: 1322-1333, 2015.
43. Peter ME, Hadji A, Murmann AE, Brockway S, Putzbach W, Pattanayak A and Ceppi P: The role of CD95 and CD95 ligand in cancer. Cell Death Differ 22: 549-559, 2015.
44. Tilsed CM, Fisher SA, Nowak AK, Lake RA and Lesterhuis WJ: Cancer chemotherapy: Insights into cellular and tumor microenvironmental mechanisms of action. Front Oncol 12: 960317, 2022.
45. Montero A, Fossella F, Hortobagyi G and Valero V: Docetaxel for treatment of solid tumours: A systematic review of clinical data. Lancet Oncol 6: 229-239, 2005.
46. Imran M, Saleem S, Chaudhuri A, Ali J and Baboota S: Docetaxel: An update on its molecular mechanisms, therapeutic trajectory and nanotechnology in the treatment of breast, lung and prostate cancer. J Drug Delivery Sci Technol: 60, 2020.
47. Sangfelt O, Erickson S and Grander D: Mechanisms of interferon-induced cell cycle arrest Front Biosci 5: D479-D487, 2000.
48. Kulkarni A, Scully TJ and O'Donnell LA: The antiviral cytokine interferon-gamma restricts neural stem/progenitor cell proliferation through activation of STAT1 and modulation of retinoblastoma protein phosphorylation. J Neurosci Res 95: 1582-1601, 2017.
49. Xaus J, Cardo M, Valledor AF, Soler C, Lloberas J and Celada A: Interferon gamma induces the expression of p21waf-1 and arrests macrophage cell cycle, preventing induction of apoptosis. Immunity 11: 103-113, 1999.
50. Bossennec M, Di Roio A, Caux C and Menetrier-Caux C: MDR1 in immunity: Friend or foe? Oncoimmunology 7: e1499388, 2018.
51. Cao ZH, Zheng QY, Li GQ, Hu XB, Feng SL, Xu GL and Zhang KQ: STAT1-mediated down-regulation of Bcl-2 expression is involved in IFN-γ/TNF-α-induced apoptosis in NIT-1 cells. PLoS One 10: e0120921, 2015. Cheon H and Stark GR: Unphosphorylated STAT1 prolongs the expression of Interferon-induced immune regulatory genes. Proc Natl Acad Sci USA 106: 9373-9378, 2009.
52. Morrow AN, Schmeisser H, Tsuno T and Zoon KC: A novel role for IFN-stimulated gene factor 3II in IFN-γ signaling and induction of antiviral activity in human cells. J Immunol 186: 1685-1693, 2011.
53. Clark DN, O'Neil SM, Xu L, Steppe JT, Savage JT, Raghunathan K and Filiano AJ: Prolonged STAT1 activation in neurons drives a pathological transcriptional response. J Neuroimmunol 382: 578168, 2023.
54. Yuasa K, Masubuchi A, Okada T, Shinya M, Inomata Y, Kida H, Shyouji S, Ichikawa H, Takahashi T, Muroi M and Hijikata T: Interferon-dependent expression of the human STAT1 gene requires a distal regulatory region located approximately 6 kb upstream for its autoregulatory system. Genes Cells 30: e13188, 2025.
55. Lastovicka J, Rataj M and Bartunkova J: Assessment of lymphocyte proliferation for diagnostic purpose: Comparison of CFSE staining, Ki-67 expression and 3H-thymidine incorporation. Hum Immunol 77: 1215-1222, 2016.
56. Zhou F: Molecular mechanisms of IFN-gamma to up-regulate MHC class I antigen processing and presentation. Int Rev Immunol 28: 239-260, 2009.
57. Steimle V, Siegrist CA, Mottet A, Lisowska-Grospierre B and Mach B: Regulation of MHC class II expression by interferon-gamma mediated by the transactivator gene CIITA. Science 265: 106-109, 1994.
58. Benesova I, Kalkusova K, Kwon YS, Taborska P, Stakheev D, Krausova K, Smetanova J, Ozaniak A, Bartunkova J, Smrž D and Strizova ZO: Cancer-associated fibroblasts in human malignancies, with a particular emphasis on sarcomas (review). Int J Oncol 67: 79, 2025.
59. Hennequin C, Giocanti N and Favaudon V: S-phase specificity of cell killing by docetaxel (Taxotere) in synchronised HeLa cells. Br J Cancer 71: 1194-1198, 1995.
60. Mosca L, Ilari A, Fazi F, Assaraf YG and Colotti G: Taxanes in cancer treatment: Activity, chemoresistance and its overcoming. Drug Resist Updat 54: 100742, 2021.
61. Tomasz M: Mitomycin C: Small, fast and deadly (but very selective). Chem Biol 2: 575-579, 1995.
62. Paz MM, Zhang X, Lu J and Holmgren A: A new mechanism of action for the anticancer drug mitomycin C: Mechanism-based inhibition of thioredoxin reductase. Chem Res Toxicol 25: 1502-1511, 2012.
63. Sritharan S and Sivalingam N: A comprehensive review on Time-tested anticancer drug doxorubicin. Life Sci 278: 119527, 2021.
64. Yosri M, Dokhan M, Aboagye E, Al Moussawy M and Abdelsamed HA: Mechanisms governing bystander activation of T cells. Front Immunol 15: 1465889, 2024.
65. Wilczynski B, Dabrowska A, Kulbacka J and Baczynska D: Chemoresistance and the tumor microenvironment: The critical role of cell-cell communication. Cell Commun Signal 22: 486, 2024.
66. Alsaafeen BH, Ali BR and Elkord E: Resistance mechanisms to immune checkpoint inhibitors: Updated insights. Mol Cancer 24: 20, 2025.
67. Ito T, Smrž D, Jung MY, Bandara G, Desai A, Smržová Š, Kuehn HS, Beaven MA, Metcalfe DD and Gilfillan AM: Stem cell factor programs the mast cell activation phenotype. J Immunol 188: 5428-5437, 2012.
68. Jung MY, Smrž D, Desai A, Bandara G, Ito T, Iwaki S, Kang JH, Andrade MV, Hilderbrand SC, Brown JM, *et al*: IL-33 induces a hyporesponsive phenotype in human and mouse mast cells. J Immunol 190: 531-538, 2013.
69. Desai A, Jung MY, Olivera A, Gilfillan AM, Prussin C, Kirshenbaum AS, Beaven MA and Metcalfe DD: IL-6 promotes an increase in human mast cell numbers and reactivity through suppression of suppressor of cytokine signaling 3. J Allergy Clin Immunol 137: 1863-1871 e1866, 2016.
70. Chang TH and Ho PC: Interferon-driven metabolic reprogramming and tumor microenvironment remodeling. Immune Netw 25: e8, 2025.

71. Wawrzyniak P and Hartman ML: Dual role of interferon-gamma in the response of melanoma patients to immunotherapy with immune checkpoint inhibitors. Mol Cancer 24: 89, 2025.
72. Nigam M, Mishra AP, Deb VK, Dimri DB, Tiwari V, Bungau SG, Bungau AF and Radu AF: Evaluation of the association of chronic inflammation and cancer: Insights and implications. Biomed Pharmacother 164: 115015, 2023.
73. Zemek RM, Chin WL, Nowak AK, Millward MJ, Lake RA and Lesterhuis WJ: Sensitizing the tumor microenvironment to immune checkpoint therapy. Front Immunol 11: 223, 2020.
74. Gillet JP, Efferth T and Remacle J: Chemotherapy-induced resistance by ATP-binding cassette transporter genes. Biochim Biophys Acta 1775: 237-262, 2007.
75. Wang X, Long M, Dong K, Lin F, Weng Y, Ouyang Y, Liu L, Wei J, Chen X, He T and Zhang HZ: Chemotherapy agents-induced immunoresistance in lung cancer cells could be reversed by trop-2 inhibition in vitro and in vivo by interaction with MAPK signaling pathway. Cancer Biol Ther 14: 1123-1132, 2013.
76. Alizadeh D, Wong RA, Gholamin S, Maker M, Aftabizadeh M, Yang X, Pecoraro JR, Jeppson JD, Wang D, Aguilar B, *et al*: IFNγ is critical for CAR T Cell-mediated myeloid activation and induction of endogenous immunity. Cancer Discov 11: 2248-2265, 2021.
77. Xu H, Niu M, Yuan X, Wu K and Liu A: CD44 as a tumor biomarker and therapeutic target. Exp Hematol Oncol 9: 36, 2020.
78. Qu S, Jiao Z, Lu G, Xu J, Yao B, Wang T, Wang J, Yao Y, Yan X, Wang T, *et al*: Human lung adenocarcinoma CD47 is upregulated by interferon-γ and promotes tumor metastasis. Mol Ther Oncol 25: 276-287, 2022.
79. Zhao Y, Shi F, Zhou Q, Li Y, Wu J, Wang R and Song Q: Prognostic significance of PD-L1 in advanced non-small cell lung carcinoma. Medicine (Baltimore) 99: e23172, 2020.
80. Lin YM, Sung WW, Hsieh MJ, Tsai SC, Lai HW, Yang SM, Shen KH, Chen MK, Lee H, Yeh KT and Chen CJ: High PD-L1 expression correlates with metastasis and poor prognosis in oral squamous cell carcinoma. PLoS One 10: e0142656, 2015.
81. Klement JD, Redd PS, Lu C, Merting AD, Poschel DB, Yang D, Savage NM, Zhou G, Munn DH, Fallon PG and Liu K: Tumor PD-L1 engages myeloid PD-1 to suppress type I interferon to impair cytotoxic T lymphocyte recruitment. Cancer Cell 41: 620-636.e9, 2023.
82. Qadir AS, Ceppi P, Brockway S, Law C, Mu L, Khodarev NN, Kim J, Zhao JC, Putzbach W, Murmann AE, *et al*: CD95/Fas increases stemness in cancer cells by inducing a STAT1-dependent type I interferon response. Cell Rep 18: 2373-2386, 2017.
83. Risso V, Lafont E and Le Gallo M: Therapeutic approaches targeting CD95L/CD95 signaling in cancer and autoimmune diseases. Cell Death Dis 13: 248, 2022.
84. Dart A: Presenting fibroblasts. Nat Rev Cancer 22: 193, 2022.
85. Mortara L, Castellani P, Meazza R, Tosi G, De Lerma Barbaro A, Procopio FA, Comes A, Zardi L, Ferrini S and Accolla RS: CIITA-induced MHC class II expression in mammary adenocarcinoma leads to a Th1 polarization of the tumor microenvironment, tumor rejection, and specific antitumor memory. Clin Cancer Res 12: 3435-3443, 2006.
86. Panelli MC, Wang E, Shen S, Schluter SF, Bernstein RM, Hersh EM, Stopeck A, Gangavalli R, Barber J, Jolly D and Akporiaye ET: Interferon gamma (IFNgamma) gene transfer of an EMT6 tumor that is poorly responsive to IFNgamma stimulation: Increase in tumor immunogenicity is accompanied by induction of a mouse class II transactivator and class II MHC. Cancer Immunol Immunother 42: 99-107, 1996.
87. Forero A, Li Y, Chen D, Grizzle WE, Updike KL, Merz ND, Downs-Kelly E, Burwell TC, Vaklavas C, Buchsbaum DJ, *et al*: Expression of the MHC Class II pathway in Triple-negative breast cancer tumor cells is associated with a good prognosis and infiltrating lymphocytes. Cancer Immunol Res 4: 390-399, 2016.
88. Roemer MGM, Redd RA, Cader FZ, Pak CJ, Abdelrahman S, Ouyang J, Sasse S, Younes A, Fanale M, Santoro A, *et al*: Major histocompatibility complex class ii and programmed death ligand 1 expression predict outcome after programmed death 1 blockade in classic hodgkin lymphoma. J Clin Oncol 36: 942-950, 2018.
89. Axelrod ML, Cook RS, Johnson DB and Balko JM: Biological consequences of MHC-II Expression by tumor cells in cancer. Clin Cancer Res 25: 2392-2402, 2019.
90. Macy AM, Herrmann LM, Adams AC and Hastings KT: Major histocompatibility complex class II in the tumor microenvironment: Functions of nonprofessional antigen-presenting cells. Curr Opin Immunol 83: 102330, 2023.
91. Johnson DB, Nixon MJ, Wang Y, Wang DY, Castellanos E, Estrada MV, Ericsson-Gonzalez PI, Cote CH, Salgado R, Sanchez V, *et al*: Tumor-specific MHC-II expression drives a unique pattern of resistance to immunotherapy via LAG-3/FCRL6 engagement. JCI Insight 3: e120360, 2018.
92. Lei PJ, Pereira ER, Andersson P, Amoozgar Z, Van Wijnbergen JW, O'Melia MJ, Zhou H, Chatterjee S, Ho WW, Posada JM, *et al*: Cancer cell plasticity and MHC-II-mediated immune tolerance promote breast cancer metastasis to lymph nodes. J Exp Med 220: e20221847, 2023.
93. Shen J, Choi YL, Lee T, Kim H, Chae YK, Dulken BW, Bogdan S, Huang M, Fisher GA, Park S, *et al*: Inflamed immune phenotype predicts favorable clinical outcomes of immune checkpoint inhibitor therapy across multiple cancer types. J Immunother Cancer 12: e008339, 2024.
94. Chen S, Crabill GA, Pritchard TS, McMiller TL, Wei P, Pardoll DM, Pan F and Topalian SL: Mechanisms regulating PD-L1 expression on tumor and immune cells. J Immunother Cancer 7: 305, 2019.
95. Mimura K, Teh JL, Okayama H, Shiraishi K, Kua LF, Koh V, Smoot DT, Ashktorab H, Oike T, Suzuki Y, *et al*: PD-L1 expression is mainly regulated by interferon gamma associated with JAK-STAT pathway in gastric cancer. Cancer Sci 109: 43-53, 2018.
96. Landsberg J, Kohlmeyer J, Renn M, Bald T, Rogava M, Cron M, Fatho M, Lennerz V, Wölfel T, Hölzel M and Tüting T: Melanomas resist T-cell therapy through Inflammation-induced reversible dedifferentiation. Nature 490: 412-416, 2012.
97. Wang B, Han Y, Zhang Y, Zhao Q, Wang H, Wei J, Meng L, Xin Y and Jiang X: Overcoming acquired resistance to cancer immune checkpoint therapy: Potential strategies based on molecular mechanisms. Cell Biosci 13: 120, 2023.
98. Goddard ET, Linde MH, Srivastava S, Klug G, Shabaneh TB, Iannone S, Grzelak CA, Marsh S, Riggio AI, Shor RE, *et al*: Immune evasion of dormant disseminated tumor cells is due to their scarcity and can be overcome by T cell immunotherapies. Cancer Cell 42: 119-134.e12, 2024.
99. Yu M, Peng Z, Qin M, Liu Y, Wang J, Zhang C, Lin J, Dong T, Wang L, Li S, *et al*: Interferon-gamma induces tumor resistance to anti-PD-1 immunotherapy by promoting YAP phase separation. Mol Cell 81: 1216-1230.e9, 2021.
100. Mandai M, Hamanishi J, Abiko K, Matsumura N, Baba T and Konishi I: Dual faces of IFNγ in cancer progression: A role of PD-L1 induction in the determination of Pro- and antitumor immunity. Clin Cancer Res 22: 2329-2334, 2016.
101. Beziaud L, Young CM, Alonso AM, Norkin M, Minafra AR and Huelsken J: IFNγ-induced stem-like state of cancer cells as a driver of metastatic progression following immunotherapy. Cell Stem Cell 30: 818-831.e6, 2023.
102. 103. Gocher AM, Workman CJ and Vignali DAA: Interferon-gamma: Teammate or opponent in the tumour microenvironment? Nat Rev Immunol 22: 158-172, 2022.
103. Korentzelos D, Wells A and Clark AM: Interferon-γ increases sensitivity to chemotherapy and provides immunotherapy targets in models of metastatic Castration-resistant prostate cancer. Sci Rep 12: 6657, 2022.
104. Gupta J, Abed HS, Uthirapathy S, Kyada A, Rab SO, Shit D, Janney B, Nathiya D, Kadhim AJ and Mustafa YF: Beyond TRAIL resistance: Novel strategies for potentiating TRAIL-induced apoptosis in cancer. Exp Cell Res 450: 114619, 2025.
105. Merchant MS, Yang X, Melchionda F, Romero M, Klein R, Thiele CJ, Tsokos M, Kontny HU and Mackall CL: Interferon gamma enhances the effectiveness of tumor necrosis factor-related apoptosis-inducing ligand receptor agonists in a xenograft model of Ewing's sarcoma. Cancer Res 64: 8349-8356, 2004.
106. Johnsen JI, Pettersen I, Ponthan F, Sveinbjornsson B, Flaegstad T and Kogner P: Synergistic induction of apoptosis in neuroblastoma cells using a combination of cytostatic drugs with interferon-gamma and TRAIL. Int J Oncol 25: 1849-1857, 2004.
107. Gawrylak A, Brodaczewska K, Iwanicka-Nowicka R, Koblowska M, Synowiec A, Bodnar L, Szczylik C, Lesyng B, Stec R and Kieda C: Hypoxia alters the response of ovarian cancer cells to the mitomycin C drug. Front Cell Dev Biol 13: 1575134, 2025.
108. Strese S, Fryknas M, Larsson R and Gullbo J: Effects of hypoxia on human cancer cell line chemosensitivity. BMC Cancer 13: 331, 2013.
109. Hultman I, Haeggblom L, Rognmo I, Jansson Edqvist J, Blomberg E, Ali R, Phillips L, Sandstedt B, Kogner P, Shirazi Fard S and Ährlund-Richter L: Doxorubicin-provoked increase of mitotic activity and concomitant drain of G0-pool in therapy-resistant BE(2)-C neuroblastoma. PLoS One 13: e0190970, 2018.

110. Lyu YL, Kerrigan JE, Lin CP, Azarova AM, Tsai YC, Ban Y and Liu LF: Topoisomerase IIbeta mediated DNA double-strand breaks: Implications in doxorubicin cardiotoxicity and prevention by dexrazoxane. Cancer Res 67: 8839-8846, 2007.
111. Stronach EA, Alfraidi A, Rama N, Datler C, Studd JB, Agarwal R, Guney TG, Gourley C, Hennessy BT, Mills GB, *et al*: HDAC4-regulated STAT1 activation mediates platinum resistance in ovarian cancer. Cancer Res 71: 4412-4422, 2011.
112. Patterson SG, Wei S, Chen X, Sallman DA, Gilvary DL, Zhong B, Pow-Sang J, Yeatman T and Djeu JY: Novel role of Stat1 in the development of docetaxel resistance in prostate tumor cells. Oncogene 25: 6113-6122, 2006.
113. Zhu H, Wang Z, Xu Q, Zhang Y, Zhai Y, Bai J, Liu M, Hui Z and Xu N: Inhibition of STAT1 sensitizes renal cell carcinoma cells to radiotherapy and chemotherapy. Cancer Biol Ther 13: 401-407, 2012.
114. Suzuki K, Yokoi A, Yoshida K, Suzuki H, Kitagawa M, Asano-Inami E, Matsuo S, Yoshihara M, Tamauchi S, Yoshikawa N, *et al*: Overcoming platinum-resistant ovarian cancer targeting the activated JAK-STAT pathways via extracellular vesicles. Commun Biol 8: 1305, 2025.
115. Damen MPF, van Rheenen J and Scheele C: Targeting dormant tumor cells to prevent cancer recurrence. FEBS J 288: 6286-6303, 2021.
116. DeMichele A, Clark AS, Shea E, Bayne LJ, Sterner CJ, Rohn K, Dwyer S, Pan TC, Nivar I, Chen Y, *et al*: Targeting dormant tumor cells to prevent recurrent breast cancer: A randomized phase 2 trial. Nat Med 31: 3464-3474, 2025.
117. Li X, Lu F, Zhou J, Li X, Li Y, Ye W, Li J, Yang L, Tang S, Zhou Y, *et al*: IFNγ augments TKI efficacy by alleviating protein unfolding stress to promote GSDME-mediated pyroptosis in hepatocellular carcinoma. Cell Death Dis 16: 512, 2025.
118. Cui C, Xu C, Yang W, Chi Z, Sheng X, Si L, Xie Y, Yu J, Wang S, Yu R, *et al*: Ratio of the interferon-γ signature to the immunosuppression signature predicts anti-PD-1 therapy response in melanoma. NPJ Genom Med 6: 7, 2021.
119. Llop S, Plana M, Tous S, Ferrando-Díez A, Brenes J, Juarez M, Vidales Z, Vilajosana E, Linares I, Arribas L, *et al*: Salvage chemotherapy after progression on immunotherapy in recurrent/metastatic squamous cell head and neck carcinoma. Front Oncol 14: 1458479, 2024.
120. Reverdy T, Varnier R, de Talhouet S, Duplomb S and Bruyas A: Analysis of the benefit of salvage chemotherapy after progression on nivolumab in patients with squamous cell carcinoma of the head and neck. Oral Oncol 145: 106533, 2023.
121. Gaughan EM and Horton BJ: Outcomes from cytotoxic chemotherapy following progression on immunotherapy in metastatic melanoma: An institutional Case-series. Front Oncol 12: 855782, 2022.
122. Abdelhamid MS, Wadan AS, Saad HA, El-Dakroury WA, Hageen AW, Mohammed DH, Mourad S, Mohammed OA, Abdel-Reheim MA and Doghish AS: Nanoparticle innovations in targeted cancer therapy: Advancements in Antibody-drug conjugates. Naunyn Schmiedebergs Arch Pharmacol 398: 6369-6389, 2025.